



FULL PAPER

Design, synthesis, and molecular docking study of novel quinoline-based *bis*-chalcones as potential antitumor agents

Daniel Insuasty^{1,2} | Stephanie García² | Rodrigo Abonia²  |
 Braulio Insuasty²  | Jairo Quiroga² | Manuel Noguerras³ | Justo Cobo³ |
 Gabriela L. Borosky⁴ | Kenneth K. Laali⁵

¹Departamento de Química y Biología, División de Ciencias Básicas, Universidad del Norte, Barranquilla, Colombia

²Department of Chemistry, Research Group of Heterocyclic Compounds, Universidad del Valle, Cali, Colombia

³Departamento de Química Inorgánica y Orgánica, Universidad de Jaén, Jaén, Spain

⁴INFIQC, CONICET and Departamento de Química Teórica y Computacional, Facultad de Ciencias Químicas, Universidad Nacional de Córdoba, Ciudad Universitaria, Córdoba, Argentina

⁵Department of Chemistry, University of North Florida, Jacksonville, Florida, USA

Correspondence

Rodrigo Abonia, Department of Chemistry, Research Group of Heterocyclic Compounds, Universidad del Valle, A. A. 25360 Cali, Colombia.

Email: rodrigo.abonia@correounivalle.edu.co

Abstract

A novel series of quinoline-based symmetrical and unsymmetrical *bis*-chalcones was synthesized via a Claisen–Schmidt condensation reaction between 3-formylquinoline/quinolone derivatives with acetone or arylidene acetones, respectively, by using KOH/MeOH/H₂O as a reaction medium. Twelve of the obtained compounds were evaluated for their in vitro cytotoxic activity against 60 different human cancer cell lines according to the National Cancer Institute protocol. Among the screened compounds, the symmetrical *N*-butyl *bis*-quinolinyl-chalcone **14g** and the unsymmetrical quinolinyl-*bis*-chalcone **17o** bearing a 7-chloro-substitution on the *N*-benzylquinoline moiety and 4-hydroxy-3-methoxy substituent on the phenyl ring, respectively, exhibited the highest overall cytotoxicity against the evaluated cell lines with a GI₅₀ range of 0.16–5.45 μM, with HCT-116 (GI₅₀ = 0.16) and HT29 (GI₅₀ = 0.42 μM) (colon cancer) representing best-case scenarios. Notably, several GI₅₀ values for these compounds were lower than those of the reference drugs doxorubicin and 5-FU. Docking studies performed on selected derivatives yielded very good binding energies in the active site of proteins that participate in key carcinogenic pathways.

KEYWORDS

anticancer activity, Claisen–Schmidt condensation, molecular docking, quinoline-based *bis*-chalcones

1 | INTRODUCTION

Although there are several therapeutic modalities for cancer treatment, namely surgery, radiotherapy, or chemotherapy, the main objective is to heal this disease or prolong and improve the quality of the life of patients. Despite the availability of the above therapeutic modalities, there is still a need for new and effective agents to help fight this disease. Among the antitumor agents currently identified,

chalcone analogs (structures **1–5**, Figure 1) represent important classes of biologically active molecules.^[1,2] They are α,β -unsaturated structures (i.e., Michael acceptors) and also are precursors in the synthesis of various heterocyclic compounds.^[3–5] Chalcones have presented a broad spectrum of biological activities such as antibacterial,^[6] antifungal,^[7] antitubercular,^[8,9] anti-inflammatory,^[10] antimalarial,^[11] and antitumor,^[12] among others. It is believed that the presence of the double bond in conjugation with the carbonyl

This study was conducted in commemoration of the retirement of Prof. A. Sánchez Rodrigo.

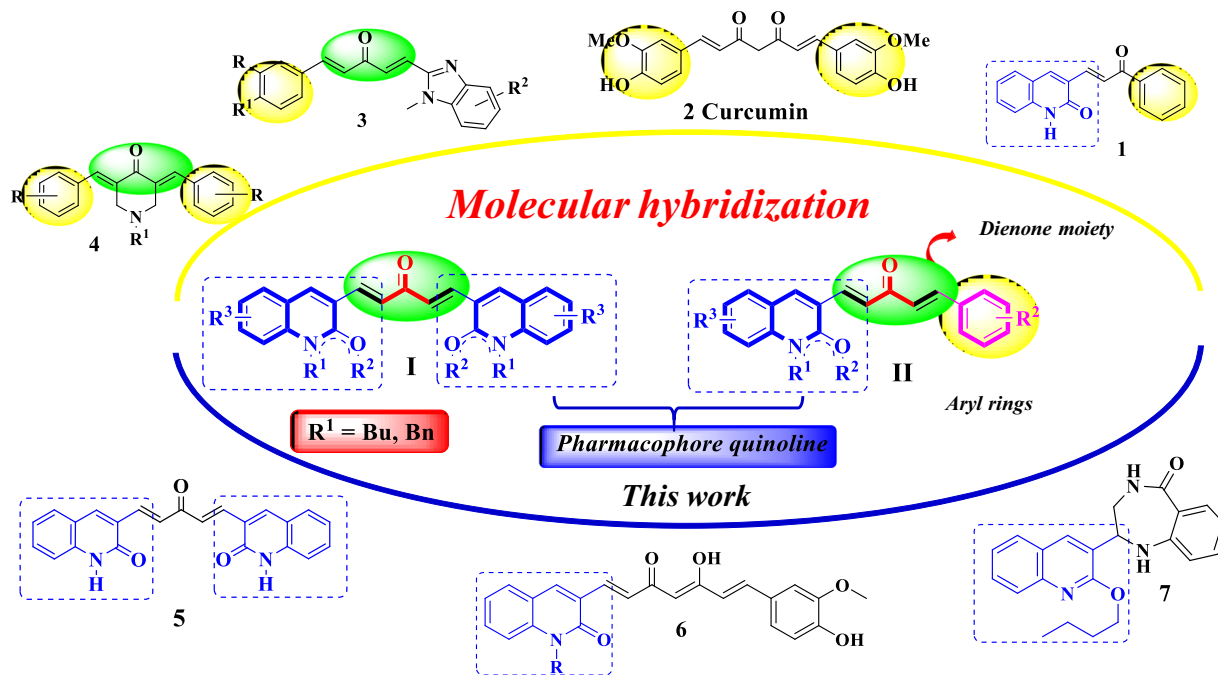


FIGURE 1 Design of new symmetrical and unsymmetrical quinoline-based bis-chalcones inspired by compound 5, curcumin, and quinolone derivatives

functionality is the main property responsible for the biological activities observed in chalcones.

Curcumin **2** is a natural component isolated from the root of the *Curcuma longa* Linn. (Zingiberaceae), which is commonly used as a dye in foods, spices, and cosmetics, as well as in traditional medicine.^[13,14] In the last few decades, curcumin has been widely studied due to its numerous biological and pharmacological activities such as antioxidant,^[15] antitumor,^[16,17] and anti-inflammatory,^[18] among others. However, its clinical use in cancer therapy has been limited due to its moderate anticancer activity, which is related to its poor bioabsorption. This limitation, along with its great chemotherapeutic potential, has inspired a large number of researchers to design and synthesize novel symmetrical and unsymmetrical curcumin-based bis-chalcones as curcumin mimetics (they should exhibit activities similar to curcumin),^[17] but, in turn, they should surpass its activity and overcome bioabsorption limitations.^[19] A variety of these derivatives (**3**, **4**, and **5**) are shown in Figure 1.^[20,21]

Quinoline is a heterocyclic system consisting of a benzene ring fused to a pyridine ring. This is a recognized pharmacophore, which is widely diffused in nature, being found in the structure of various natural products. Quinoline derivatives are useful in various practical applications including a number of pharmaceuticals available as medicines today.^[22–24] Therefore, the synthesis of these derivatives has been extensively reported by different conventional and non-conventional methods.^[2,5,25,26]

Following a fragment-based design strategy in the antitumor drug discovery,^[27] and combining the pharmacophoric fragments found in curcumin–quinolinic systems and α,β -unsaturated Michael acceptors (chalcones), we have designed new quinoline–chalcone

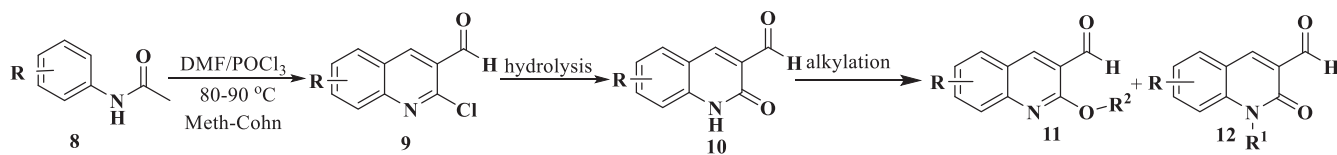
hybrids such as quinoline–curcuminoid analog **5**, as depicted in Figure 1, which has been recently reported by our research group. This compound showed antitumor activity in studies performed by the National Cancer Institute (NCI).^[2] These promising results encouraged us to continue the synthesis of new quinoline-based chalcone derivatives.^[28,29] Herein, we describe the structural modifications performed on compound **5**, in an effort to improve its biological activity. We are also describing an attempt to establish a possible structure–activity relationship supported by docking calculations, which could serve as a designing tool for the future.

2 | RESULTS AND DISCUSSION

2.1 | Chemistry

The synthetic route for the novel symmetrical and unsymmetrical bis-quinolinyl-chalcones **14** and **17** is outlined in Scheme 1 and Tables 1 and 2. The key intermediate, 2-chloroquinoline-3-carbaldehyde **9**, was prepared by following our previously reported methodology,^[30] which involved a Meth–Cohn-type reaction,^[31] followed by hydrolysis and alkylation processes to afford the substituted 3-formylquinolines (**10–12**) (Scheme 1).

Then, the symmetrical bis-quinolinyl-chalcones **14a–k** were synthesized via a Claisen–Schmidt condensation reaction between two equivalents of the differently substituted 3-formylquinolines (**10–12**) with one equivalent of acetone in the presence of 40% aq. KOH using a mixture of methanol/water as solvent. The reaction mixture was stirred at ambient temperature, and after completion, it



SCHEME 1 Synthesis of 2-chloroquinoline-3-carbaldehyde **9** and its conversion to 3-formylquinolines **10–12**. DMF, dimethylformamide

was neutralized with acetic acid and the crudes were purified by recrystallization or column chromatography on silica gel. In all cases, the reactions proceeded with the same behavior, affording the expected *bis*-quinolinyl-chalcones **14a–k** in good to excellent yields (Table 1).

The structure of the symmetrical *bis*-quinolinyl-chalcone **14** was ascertained by infrared (IR), 1D and 2D nuclear magnetic resonance (NMR) (in dimethyl sulfoxide [DMSO]- d_6), and mass spectrometric analysis. Taking compound **14a** as model, in the ^1H NMR spectrum, a singlet observed at 2.52 ppm was assigned to the CH_3 protons. Two doublets at 7.74 and 7.81 ppm with coupling constant $J = 15.9$ Hz were assigned to the vinylic protons (H_α and H_β , Table 1), confirming the *E* configuration of the new double bonds formed. Two doublets and two singlets, integrating for a total of eight protons, corresponded to the C–H protons of the quinolin-2-onyl moiety. The ^{13}C NMR spectrum showed signals for 13 carbons (corresponding to one methyl, six methine, and six quaternary carbon atoms) in agreement with structure **14a**. Finally, the IR spectrum exhibited absorptions at 3154 cm^{-1} assigned to the NH functionality and two $\text{C}=\text{O}$ absorptions at 1661 and 1659 cm^{-1} .

The synthesis of the unsymmetrical quinolinyl-*bis*-chalcones **17a–w** was performed in two steps. Initially, the arylidene acetones **16a–d** were prepared by simple aldol condensation between benzaldehydes **15a–d** and an excess of acetone at 0°C . In the second step, crude products **16a–d** were condensed with the respective 3-formylquinolines **10–12** in similar fashion but at ambient temperature to furnish the desired unsymmetrical quinolinyl-*bis*-chalcones **17a–w** in satisfactory yields (Table 2).

The structures of the new compounds **17a–w** were also consistent with their spectral data IR, 1D and 2D NMR, mass spectrometry, and microanalysis, and they are summarized in Section 4.

2.2 | Anticancer activity evaluation

The new quinolinyl-chalcones **14** and **17** were submitted to the Developmental Therapeutics Program (DTP) at NCI, Bethesda, MD, USA, for in vitro anticancer screening against 60 human cell lines corresponding to nine human cancer panels: leukemia, non-small-cell lung, melanoma, colon, central nervous system (CNS), ovary, renal, breast, and prostate cancer.^[32] The process started with a primary in vitro evaluation against the 60 human tumor cell lines at a single dose of $10\text{ }\mu\text{M}$ for 12 selected compounds (i.e., **14g** (NSC: D-796113/1), **17b** (NSC: 768474/1), **17c** (NSC: 768473/1), **17d** (NSC: D-796114/1), **17e** (NSC: D-787549/1), **17j** (NSC: D-789980/1), **17m**

(NSC: D-796110/1), **17n** (NSC: D-796111/1), **17o** (NSC: D-796112/1), **17s** (NSC: D-789977/1), **17v** (NSC: D-789976/1), and **17w** (NSC: D-796109/1)). The obtained results for each compound are reported in NCI one-dose mean graphs as growth percent (GP) (negative values mean lethality, see Supporting Information) and mean and range values of the tested cell (see Supporting Information). Table 3 summarizes the most remarkable results for the evaluated compounds in terms of growth inhibition percentage ($\text{GI}\% = 100 - \text{GP}$), lethality (values shown in parentheses), and mean values.

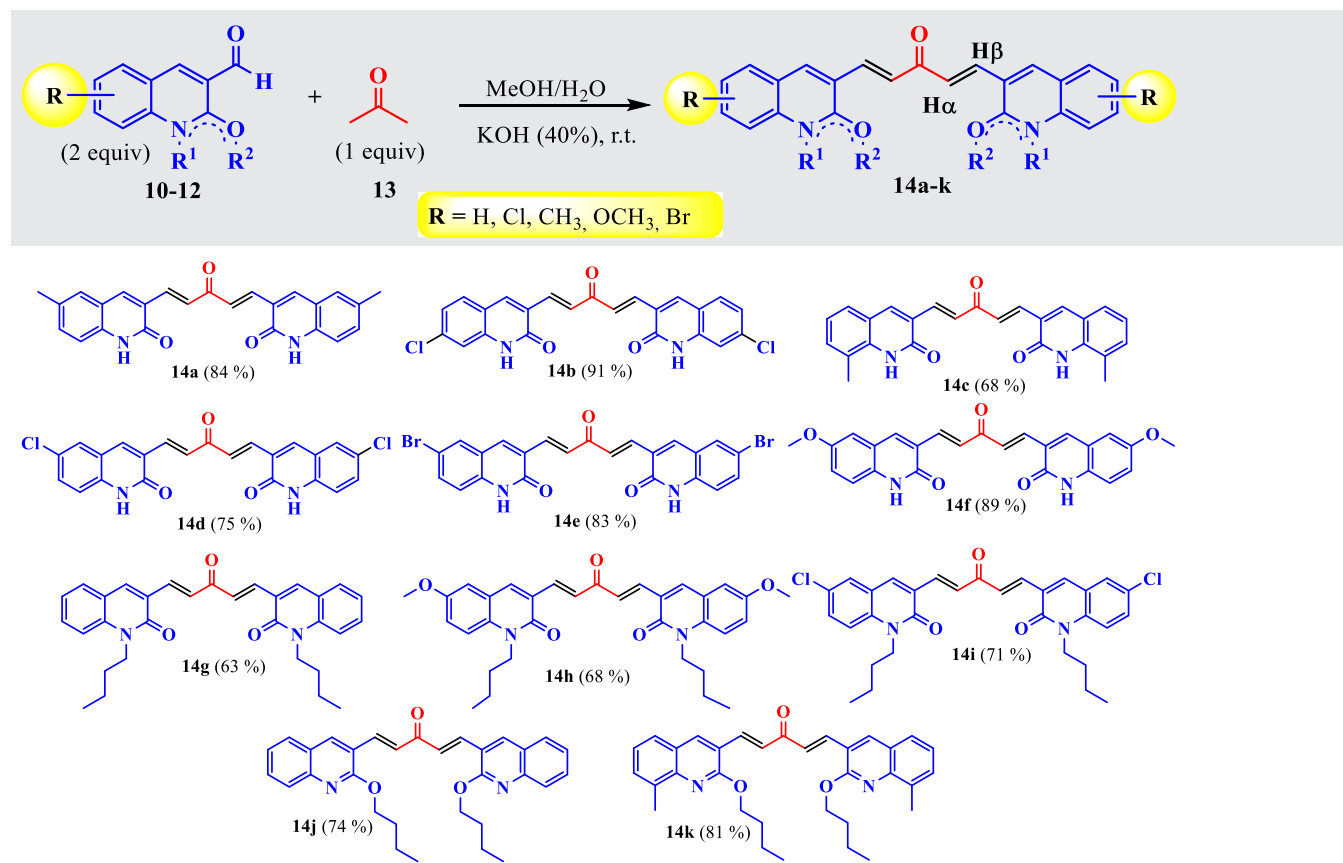
According to the data analysis of the one-dose mean graphs, low GP values afford better growth inhibition ($\text{GI}\%$) results because $\text{GI} = 100 - \text{GP}$. As negative values correspond to lethal activity, hence, values that are more negative represent higher activity of the assayed compound (see Supporting Information). In addition, low mean values represent better activity; indeed, mean values ≤ 50 indicate that the compound is active. Moderately active compounds afford mean values around 50–60. Thus, in terms of the lower (GP and mean) and higher ($\text{GI}\%$ and lethality) values for one-dose criteria, among the 12 quinolinyl-chalcones evaluated, five of them were active (i.e., **14g**, **17d**, **17e**, **17n**, and **17o**), whereas three compounds were moderately active (i.e., **17b**, **17c**, and **17m**), as shown in Table 3.

As the abovementioned compounds displayed the highest anti-proliferative activity at one-dose assays, they were selected by NCI for advanced assays against the full 60 human cell lines at five different concentrations (five-dose assay) (i.e., 100, 10, 1.0, 0.1, and $0.001\text{ }\mu\text{M}$), through a protocol in which sulforhodamine B (SRB) protein is used to estimate the cell growth.^[33,34] The results were expressed in GI_{50} and LC_{50} values, and they are summarized in Table 4.

In general, the selected quinolinyl-chalcones displayed moderate to excellent activity against the evaluated cell lines, with several of them having GI_{50} values lower than $1.00\text{ }\mu\text{M}$ (red color values). Compounds **17b** and **17c** displayed a moderate activity against the evaluated cancer cell lines, with HCT-116 (colon) and MCF7 (breast) cancer cell lines being the most sensitive strains, with GI_{50} of 1.55 and $0.92\text{ }\mu\text{M}$, respectively. The quinolinyl-*bis*-chalcone **17e** showed better activity against RPMI-8226 (leukemia), HCT-116 (colon), and MCF7 (breast) cancer cell lines with GI_{50} values of 0.33, 0.26, and $0.36\text{ }\mu\text{M}$, respectively, whereas compound **17n** displayed considerable cytotoxic activity against HT29 (colon) with GI_{50} of $0.85\text{ }\mu\text{M}$.

Compound **17d** was found to be highly sensitive against RPMI-8226 ($\text{GI}_{50} = 0.36\text{ }\mu\text{M}$, leukemia), SR ($\text{GI}_{50} = 0.38\text{ }\mu\text{M}$, leukemia), HCT-116 ($\text{GI}_{50} = 0.16\text{ }\mu\text{M}$, colon), HT29 ($\text{GI}_{50} = 0.78\text{ }\mu\text{M}$, colon), MDA-MB-435 ($\text{GI}_{50} = 0.30\text{ }\mu\text{M}$, melanoma), and MCF7 ($\text{GI}_{50} = 0.39$

TABLE 1 Synthesis of symmetrical bis-quinoliny-chalcones 14a–k



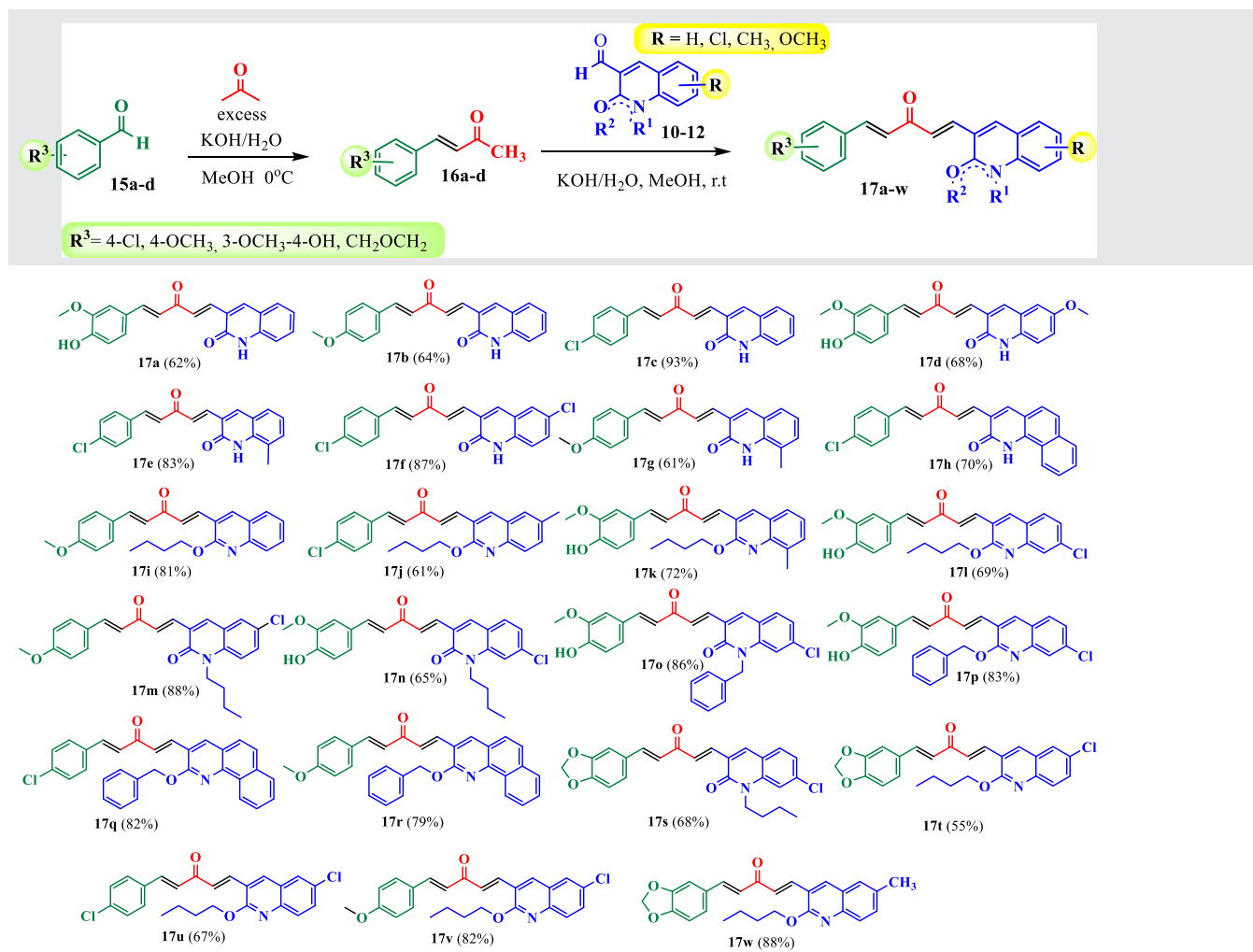
μM, breast), whereas the quinoliny-bis-chalcone **17o** showed better results against SR (GI₅₀ = 0.46 μM, leukemia), HCT-116 (GI₅₀ = 0.77 μM, colon), HT29 (GI₅₀ = 0.42 μM, colon), MDA-MB-435 (GI₅₀ = 0.86 μM, melanoma), OVCAR-3 (GI₅₀ = 0.71 μM, ovarian), OVCAR-8 (GI₅₀ = 0.50 μM, ovarian), and MCF7 (GI₅₀ = 0.42 μM, breast). Indeed, **17d** and **17o** displayed significant cytotoxic activity against all screened cell lines with GI₅₀ values varying from 0.16 to 5.95 μM.

However, the symmetrical bis-quinoliny-chalcone **14g** exhibited potent anticancer activity against all 60 tested cancer cell lines, 12 of them, with GI₅₀ values ≤ 1.00 μM. Compound **14g** showed significant activity against the leukemia cell lines K-562 (GI₅₀ = 0.88 μM), RPMI-8226 (GI₅₀ = 0.32 μM), and SR (GI₅₀ = 0.32 μM), Colon cancer cell lines HT29 (GI₅₀ = 0.32 μM), KM12 (GI₅₀ = 0.68 μM), and SW-620 (GI₅₀ = 0.86 μM), melanoma cell line M14 (GI₅₀ = 0.45 μM), and breast cancer cell lines MCF7 (GI₅₀ = 0.31 μM) and BT-549 (GI₅₀ = 0.70 μM). However, the best cytostatic activity of compound **14g** was displayed against the HCT-116 (colon) cancer cell line, with GI₅₀ = 0.16 μM, and MDA-MB-435 (melanoma) cell line, with GI₅₀ = 0.21 μM. It is also worth mentioning that the evaluated chalcones showed better GI₅₀ values than the reference drug 5-FU in 107 cases (blue background values) and better GI₅₀ values than the reference drug doxorubicin in 11 cases (gray background values), as shown in Table 4.

In addition, mean GI₅₀ values (per cancer cell panel) were determined for six chalcones (**14g** and **17b–d,n,o**) to be compared with those for the standard anticancer agents doxorubicin and 5-FU. For a better understanding, the values were drawn and depicted in Figure 2 (compound **17e** was omitted in this analysis due to its lower activity and lack of several GI₅₀ data). According to Figure 2, the symmetrical bis-quinoliny-chalcone **14d** displayed higher activity against almost all panels (six of them) in comparison with the remaining evaluated chalcones **17**. Indeed, based on the number of hits per panels, the order of activity of the evaluated chalcones would be as follows: **14g** > **17d** ≈ **17o** > **17n** > **17b** > **17c**. Compound **14g** also displayed higher activity against most panels (except for colon and CNS) than the standard drug 5-FU and even was more active than the standard drug doxorubicin for the colon panel. Remarkably, the six evaluated chalcones displayed higher activity in four panels (non-small-cell lung, melanoma, renal, and breast cancer) than the standard drug 5-FU. It is worth mentioning that the quinoliny-bis-chalcones **17d,o** also afforded outstanding mean GI₅₀ values in each panel, with seven of them being better than the standard drug 5-FU in both cases.

The above findings indicate that the symmetrical bis-quinoliny-chalcone **14g** and the unsymmetrical quinoliny-bis-chalcone **17o** are most superior among the structures of the evaluated series, reflecting that such compounds might be used as promising lead molecules for discovering a new class of anticancer agents.

TABLE 2 Synthesis of unsymmetrical quinolinyl-bis-chalcones 17a-w



2.3 | Computational docking studies

Molecular docking calculations for quinolinyl-chalcones **14g** and **17b-e,n,o** were carried out with the aim to elucidate the factors influencing their bioactivities. Selection of these representative compounds was made according to their higher (**14g**, **17d,o**) and moderate (**17b,c,e,n**) anticancer activity determined *in vitro*. The binding energies of these compounds in the active site of various proteins involved in carcinogenic processes were determined and compared with the binding affinities of known inhibitors employed in chemotherapy. The proteins selected for these docking studies participate in diverse oncogenic pathways, which were described in previous works.^[35] Very good correspondences were observed between the binding modes obtained in the present computations and the crystallographic structures of the complexes for the reference inhibitors (PDB codes are shown in Table 5). This accordance supports the validation of the docking protocol applied.

As a general observation, the studied selected compounds docked properly in the binding pockets of the considered enzymes and afforded very good binding energies. The main interactions between these ligands and the proteins were hydrophobic; however,

some hydrogen bonds were also observed (Figure 3). Most of the obtained docking affinities were comparable to or even better than those of usually applied anticancer drugs (Table 5). As the selected chalcones docked in the same binding site of the receptors as the known inhibitors, and presented significant binding scores, these computational results, thus, indicate the studied derivatives as potential new anticancer agents. In particular, HER1, HER2, proteasome, and hTS appear as promising targets for these compounds.

Considering the remarkable anticancer activity exhibited by *bis*-chalcones **14g** and **17o** in the described *in vitro* studies, the binding interactions of these molecules were analyzed and compared with some reference inhibitors. The *bis*-chalcone **14g** showed its best cytostatic activity against CRC cell lines; interestingly, this molecule yielded a more favorable binding affinity than the known HER1 inhibitors (Table 5). Comparison of the binding interactions of **14g** and gefitinib in HER1 showed common interactions with nine residues (Figure 4). Derivative **14g** presented only hydrophobic contacts, whereas one hydrogen bond was observed between gefitinib and Met793. The more favorable binding energy of **14g** could be ascribed to its bigger volume, which enabled this molecule to interact with 13 amino acids, whereas gefitinib made contacts with 11 residues.

TABLE 3 In vitro growth inhibition percentages (GI%) and lethality caused by the tested compounds at one dose of 10 µM for representative cell lines

Cell line	GI% and lethality values at 10 µM ^{a,b}													
	14g	17b	17c	17d	17e	17j	17m	17n	17o	17s	17v	17w		
<i>Leukemia</i>														
RPMI-8226	100 (32.1)	100 (22.0)	100 (22.2)	100 (18.5)	94	69	100 (18.8)	100 (14.2)	100 (18.8)	0	91.1	95		
SR	98.2	100 (2.1)	98.2	98.7	99.4	0	96.8	96.2	98.2	0	23.8	57.1		
<i>Non-small-cell lung cancer</i>														
A549/ATCC	100 (0.94)	48.7	53.5	77.4	34.4	28.2	48.9	73.6	100 (4.0)	18.2	7.9	21.7		
NCI-H226	100 (22.8)	9.1	6.5	63.2	37.9	5.8	30	100 (18.4)	100 (6.1)	1.5	0.4	3.7		
NCI-H23	100 (7.4)	29.6	32	94.6	37.2	0.9	51.4	72.3	100 (20.6)	0	4.1	17.6		
NCI-H522	94.3	51.2	53.6	71	51.7	31.8	43.8	100 (44.0)	100 (37.6)	17.8	22.5	39.4		
<i>Colon cancer</i>														
HCC-2998	100 (92.6)	3.3	27	100 (74.0)	100 (4.9)	0	9.4	66.7	100 (73.8)	0	7.3	0		
HCT-116	100 (90.6)	100 (30.8)	100 (55.7)	100 (86.7)	100 (52.7)	64.6	100 (67.1)	100 (55.5)	100 (82.6)	7.9	100 (25.4)	89.5		
HT29	100	96.3	100 (0.3)	100 (38.6)	92.2	17	90.3	100 (41.7)	100 (46.5)	8.9	28.4	36.4		
KM12	100 (75.9)	72.4	71.7	100 (45.0)	91.6	10.2	74.1	93.2	100 (52.3)	2.6	16	12.7		
SW-620	100 (2.9)	63.6	91.5	100 (24.8)	91.5	0	81.7	83.9	96.6	0	0	0.5		
<i>CNS cancer</i>														
SF-295	96.4	0	100 (1.8)	82.5	16.2	0	80.1	69.8	94.1	0	0	0		
SF-539	100 (7.13)	0	100	91.5	30.3	0.8	8.2	47.5	90.1	0	0	0		
U251	100 (48.3)	86.3	88.3	100 (13.0)	89.4	15.9	100 (13.4)	96.7	100 (64.7)	3.41	19.5	51.7		
<i>Melanoma</i>														
LOX IMVI	100 (80.3)	100 (21.0)	100 (44.5)	100 (36.0)	95.8	13.8	90.8	100 (51.3)	100 (90.0)	1.1	28.5	22.7		
M14	100 (28.8)	27.1	39.7	100 (32.4)	69.5	0	5	94.9	100 (11.3)	0	33.7	47.6		
MDA-MB-435	100 (65.2)	86.4	100 (1.7)	100 (30.0)	100 (32.7)	30.4	4.4	97.2	100 (19.1)	0	90.4	64.2		
SK-MEL-5	100 (74.4)	13.3	24.8	90.6	0	0	21.1	96.6	100 (80.5)	0	6.1	22.4		
UACC-257	100 (24.0)	25.2	11.1	59.7	8.8	28.2	7.9	67.9	100 (13.8)	6.9	10.4	26.7		
UACC-62	100 (43.8)	46.5	47.1	89.2	69.6	16	23.8	97.6	100 (56.0)	6.6	21.1	24.4		

TABLE 3 (Continued)

Cell line	GI% and lethality values at 10 μM ^{a,b}													
	14g	17b	17c	17d	17e	17j	17m	17n	17o	17s	17v	17w		
<i>Ovarian cancer</i>														
OVCAR-3	100 (15.7)	68	84.1	100 (11.2)	86.1	2.3	80.5	100 (26.2)	100 (46.4)	2.8	1.8	25.4		
OVCAR-8	100 (0.9)	100 (11.8)	100 (11.5)	98.6	78.2	6.7	94.8	100 (4.0)	94.4	0	3.8	61.3		
<i>Renal cancer</i>														
786-0	100 (63.0)	6.8	11.5	100 (42.7)	85.5	0	71.7	100 (0.5)	100 (55.7)	0	0	2.1		
ACHN	94.3	15.9	26	50.1	39.5	2.9	0	80.1	100 (15.4)	0	0	0		
RXF 393	100 (89.9)	69.4	61.7	100 (76.7)	63.2	0	15.5	100 (15.0)	100 (79.9)	0	0.9	0		
SN12C	100 (28.2)	33.5	37.2	95.3	52.4	0	24.1	87.7	100 (18.4)	0	0	10.8		
UO-31	100 (95.2)	5.6	36.1	100 (70.8)	30.4	15.5	37.2	94	100 (88.9)	17.4	15.6	25		
<i>Prostate cancer</i>														
PC-3	98.5	47.7	51.2	90.5	66.2	10.3	60.5	72.8	100 (2.4)	4.4	11.1	27.6		
DU-145	100 (1.5)	18.8	20.7	91.7	60.9	0	46.5	80.7	100 (35.1)	0	6.2	17.2		
<i>Breast cancer</i>														
MCF7	98.5	85.5	94.8	87.1	90.1	64.4	65.6	53.7	73.8	4.6	69.3	62.2		
MDA-MB-231/ATCC	100 (8.0)	35.5	36.2	81.7	74.3	4.4	16.2	100 (11.2)	100 (16.7)	0	0	7.2		
BT-549	100 (7.9)	35.1	55.4	100 (22.8)	92.7	8.5	10.6	88.6	100 (19.2)	0	6.4	24.1		
MDA-MB-468	100 (8.0)	56.1	44.1	100 (32.1)	38.3	0	13.9	85	100 (42.8)	0	0	4.1		
Mean ^c	-11.73	59.31	53.66	12.43	45.78	93.2	58.73	18.19	-13.20	101.8	89.45	82.93		

^aInhibition values of the most sensitive cell lines against the assayed compounds are highlighted in bold.^bLethality percentages are represented in parentheses and were obtained from the original NCI one-dose mean graphs.^cThe mean values are obtained from the original NCI one-dose mean graphs.

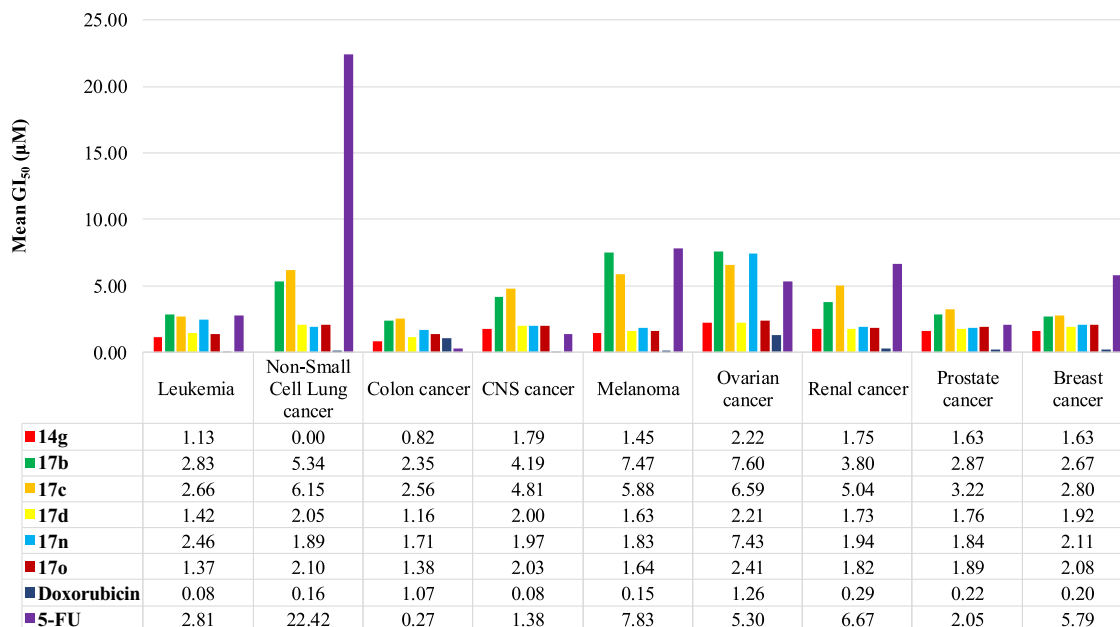


FIGURE 2 Comparison of the mean GI_{50} values, per panel, displayed by chalcones **14g**, **17b–d,n,o**, and the standard drugs doxorubicin and 5-fluorouracil (5-FU) against the 60 human cancer cell lines

The unsymmetrical *bis*-chalcone **17o** exhibited an excellent *in vitro* activity against leukemia cell lines. In accordance with these observations, this compound presented a clearly superior binding affinity to Bcl-2 as compared with the reference chemotherapeutic drugs (Table 5). Inspection of the binding modes of **17o** and navitoclax in the active site of Bcl-2 revealed common interactions with 12 residues (Figure 5). Most of the interactions were hydrophobic, with the exception of one hydrogen bond with Ala97 in the case of **17o** and with Gly142 for navitoclax. This hydrogen-bond contact was slightly shorter for **17o** (the distance between heavy atoms was 3.07 Å) than for navitoclax (3.14 Å). This stronger interaction would explain the improved binding affinity of **17o**. According to this, docking calculations point to the 4-hydroxy-3-methoxy-substituted phenyl ring as the main pharmacophoric moiety for this *bis*-chalcone derivative.

3 | CONCLUSION

In summary, a series of new symmetrical and unsymmetrical quinoline-based *bis*-chalcones was prepared and characterized. Twelve of them were subjected to *in vitro* anticancer screening, against 60 NCI human cancer cell lines at a single concentration of 10^{-5} M (one dose). Compounds **14g**, **17d**, **17e**, **17n**, and **17o** were most active, whereas compounds **17b**, **17c**, and **17m** were moderately active. Subsequently, compounds (**14g** and **17b–e,n,o**) were evaluated at five different concentrations (five doses), and among them, the symmetrical *N*-butylquinolin-chalcone **14g** and the unsymmetrical *bis*-chalcone **17o** exhibited the highest cytotoxicity with an overall GI_{50} value range of 0.16–5.45 μ M, with HCT-116 (GI_{50} = 0.16) and HT29 (GI_{50} = 0.42 μ M) (colon cancer) being exceptionally active. Remarkably, several GI_{50} values for these compounds were better than those for the reference drugs

doxorubicin and 5-FU. In addition, molecular docking calculations for six of the studied compounds exhibited remarkable binding affinities (mainly compounds **17o** and **14g**) in the binding pockets of several enzymes involved in carcinogenesis. Most of the observed binding energies were comparable to or even superior to the values obtained for known anticancer drugs typically employed in chemotherapy. Analysis of the binding modes of compounds **17o** and **14g** in selected protein active sites revealed several interactions in common with some reference inhibitors. Moreover, these studied derivatives presented stronger binding interactions as compared with the known chemotherapeutic drugs, suggesting they could be potential new anticancer agents.

4 | EXPERIMENTAL

4.1 | Chemistry

4.1.1 | General

All organic chemicals and solvents were procured from Sigma-Aldrich, Fluka, and Merck (analytical grade reagent), and used without further purification. IR spectra were recorded on a Shimadzu FTIR 8400 ATR spectrophotometer. Melting points were measured using a Stuart SMP3 melting point apparatus and were uncorrected. ^1H and ^{13}C NMR spectra (see the Supporting Information) were recorded on a Bruker Avance 400 spectrophotometer operating at 400 and 100 MHz, respectively, using $\text{DMSO-}d_6$ and CDCl_3 as solvents and tetramethylsilane as the internal standard. Mass spectra were run on a SHIMADZU-GCMS 2010-DI-2010 spectrometer (equipped with a direct inlet probe) operating at 70 eV. Microanalyses were performed on an Agilent CHNS

TABLE 4 In vitro cytotoxic activities for compounds **14g** and **17b–e,n,o** expressed as 50% of growth inhibition and lethal concentration, against 60 human cancer cell lines, compared with the standard drugs doxorubicin and 5-fluorouracil (5-FU)^a

Panel cell line	Compounds														Reference drugs				
	14g		17b		17c		17d		17e		17n		17o		Doxorubicin ^d		5-FU		
	GI ₅₀ (μ M)	LC ₅₀ (μ M)	GI ₅₀ (μ M)	LC ₅₀ (μ M)	GI ₅₀ (μ M)	LC ₅₀ (μ M)	GI ₅₀ (μ M)	LC ₅₀ (μ M)	GI ₅₀ (μ M)	LC ₅₀ (μ M)	GI ₅₀ (μ M)	LC ₅₀ (μ M)	GI ₅₀ (μ M)	LC ₅₀ (μ M)	GI ₅₀ (μ M)	LC ₅₀ (μ M)	GI ₅₀ (μ M)	LC ₅₀ (μ M)	
Leukemia																			
CCRF-CEM	1.88	>100	2.98	>100	3.09	>100	2.06	>100	3.98	>100	2.79	>100	1.40	>100	0.08	100.00	10.00	>100	
HL-60(TB)	1.71	>100	3.24	>100	2.83	>100	2.24	>100	---	>100	2.34	>100	1.34	>100	0.12	89.33	2.51	>100	
K-562	0.88	>100	3.34	>100	---	---	1.35	>100	3.80	>100	2.82	>100	1.89	>100	0.19	100.00	3.98	>100	
MOLT-4	2.23	>100	3.20	>100	3.82	>100	2.93	>100	5.69	>100	2.17	>100	1.89	>100	0.03	100.00	0.32	>100	
RPMI-8226	0.32	>100	1.77	>100	1.29	>100	0.36	>100	0.33	>100	2.46	>100	1.23	>100	0.08	100.00	0.05	>100	
SR	0.32	>100	2.88	>100	2.42	>100	0.38	>100	2.72	>100	2.04	>100	0.46	>100	0.03	100.00	0.03	>100	
Non-Small Cell Lung cancer																			
A549/ATCC	1.56	6.44	3.16	>100	3.16	>100	2.24	34.8	---	>100	1.72	17.00	2.05	31.6	0.06	100.00	0.20	>100	
EKVX	1.88	13.0	---	---	---	---	1.95	96.9	---	---	2.18	9.63	2.11	11.1	0.41	47.97	63.10	>100	
HOP-62	2.27	7.33	4.67	59.7	8.21	73.3	2.03	13.6	100	>100	1.81	9.61	2.75	38.2	0.07	67.61	0.40	>100	
HOP-92	1.96	8.68	---	---	---	---	1.84	22.6	100	>100	1.75	10.20	2.21	>100	0.10	42.27	79.43	>100	
NCI-H226	2.51	9.42	4.42	62.5	2.59	>100	2.14	22.7	100	>100	1.77	10.40	2.02	39.8	0.05	6.40	50.12	>100	
NCI-H23	1.77	---	4.31	84.9	4.76	>100	2.04	18.1	---	>100	2.06	14.90	1.79	19.2	0.15	13.15	0.32	>100	
NCI-H322M	1.64	6.74	13.9	79.4	13.9	>100	2.44	24.9	---	>100	2.01	11.00	2.42	26.9	0.54	67.76	0.20	>100	
NCI-H460	1.80	6.76	4.98	67.1	8.52	90.8	2.04	16.9	100	>100	1.96	8.87	1.89	9.67	0.02	51.29	0.06	>100	
NCI-H522	1.86	8.91	1.97	16.1	1.91	22.8	1.74	8.62	---	>100	1.78	8.37	1.67	7.33	0.03	2.80	7.94	>100	
Colon cancer																			
COLO 205	1.41	7.09	3.31	39.7	3.65	55.0	1.60	9.09	---	>100	1.72	16.80	1.97	>100	0.18	4.33	0.16	>100	
HCC-2998	1.01	5.02	2.19	7.78	2.02	6.47	1.97	6.72	1.81	---	2.05	6.13	1.98	6.11	0.26	21.68	0.05	>100	
HCT-116	0.16	---	1.55	6.76	1.46	---	0.16	0.70	0.26	3.19	1.52	5.90	0.77	5.11	0.08	54.58	0.25	25.12	
HCT-15	1.29	6.38	2.41	>100	2.85	>100	1.41	10.8	---	>100	1.90	2.25	1.24	15.4	6.46	100.00	0.10	>100	
HT29	0.32	5.74	2.47	26.3	2.50	31.6	0.78	4.95	---	---	0.85	7.21	0.42	7.18	0.12	67.45	0.16	>100	
KM12	0.68	5.76	2.62	33.9	3.11	39.1	1.08	6.54	---	>100	1.89	7.09	1.70	7.61	0.27	92.68	0.20	>100	
SW-620	0.86	8.78	1.89	15.2	2.31	32.7	1.13	9.83	2.98	>100	2.05	9.28	1.56	17.2	0.09	58.61	1.00	>100	
CNS cancer																			
SF-268	1.98	41.7	3.11	51.6	3.61	70.7	2.25	28.8	---	>100	1.96	19.3	2.16	38.9	0.10	30.48	1.58	>100	
SF-295	1.84	97.9	2.65	38.4	3.48	62.0	2.36	34.6	---	>100	2.75	32.1	3.00	32.9	0.10	69.98	0.25	>100	
SF-539	1.47	86.6	2.63	45.8	2.88	>100	1.58	6.53	100	>100	1.62	6.24	1.62	76.9	0.12	27.23	0.06	>100	
SNB-19	1.63	6.45	10.6	79.4	11.3	54.0	1.67	9.23	---	>100	1.62	6.75	1.73	87.3	0.04	49.77	---	---	
SNB-75	2.80	>100	4.33	48.1	5.79	75.4	2.96	>100	16.8	>100	2.26	22.20	2.52	27.7	0.07	3.30	3.98	>100	
U251	1.03	4.90	1.81	7.66	1.81	7.51	1.17	6.16	2.86	>100	1.59	5.97	1.17	5.56	0.04	30.62	1.00	>100	
Melanoma																			
LOX IMVI	1.24	5.91	---	---	---	---	1.5	6.60	---	>100	1.51	5.33	1.29	5.26	0.07	50.35	0.25	79.43	
MALME-3M	2.29	16.4	9.17	>100	7.63	>100	2.16	17.5	100	>100	2.14	13.50	1.94	76.1	0.12	3.97	0.05	>100	
M14	0.45	---	2.80	64.5	3.11	>100	1.67	22.1	---	>100	1.86	9.37	1.83	23.4	0.18	4.05	1.00	>100	
MDA-MB-435	0.21	1.36	2.22	18.9	2.34	24.0	0.30	5.32	---	---	1.77	9.79	0.86	20.8	0.25	9.57	0.08	>100	
SK-MEL-2	2.09	78.2	---	---	---	---	2.47	29.9	---	>100	2.67	20.90	1.92	31.6	0.17	1.06	63.10	>100	
SK-MEL-28	1.81	6.70	13.9	86.4	10.0	68.4	1.69	6.26	100	>100	1.93	8.79	1.85	27.7	0.21	15.92	1.00	>100	
SK-MEL-5	1.77	6.06	11.0	57.2	10.1	62.5	1.77	6.01	---	>100	1.69	5.64	1.69	5.96	0.08	0.49	0.50	79.43	
UACC-257	1.61	5.61	10.8	59.2	5.20	52.7	1.58	6.06	100	>100	1.41	7.79	2.06	1.61	0.14	8.15	3.98	>100	
UACC-62	1.61	5.82	2.43	37.4	2.80	34.9	1.52	6.72	100	>100	1.48	7.08	1.29	1.25	0.12	0.74	0.50	>100	

(Continues)

Ovarian cancer																		
IGROV1	1.46	8.00	2.21	23.9	2.34	37.4	1.77	10.7	----	>100	1.92	8.77	1.74	26.4	0.17	100.00	1.26	>100
OVCAR-3	1.21	5.05	2.84	28.7	2.07	9.80	1.18	5.50	2.62	>100	1.70	6.20	0.71	7.32	0.39	84.33	0.02	50.12
OVCAR-4	2.78	>100	9.73	>100	5.06	>100	2.91	>100	100	>100	2.34	39.9	2.48	>100	0.37	74.30	3.98	>100
OVCAR-5	1.96	7.23	5.13	68.9	4.65	74.3	1.88	7.13	100	>100	2.57	9.31	2.65	23.1	0.41	100.00	10.00	>100
OVCAR-8	1.50	>100	3.55	>100	3.03	>100	1.52	95.6	----	>100	2.47	30.9	0.50	>100	0.10	43.25	1.58	>100
NCI/ADR-RES	3.01	>100	20.5	>100	16.8	>100	3.39	>100	100	>100	2.90	53.6	2.86	>100	7.16	100.00	0.32	>100
SK-OV-3	3.59	>100	9.22	74.0	12.2	87.6	2.79	42.6	100	>100	38.1	45.9	5.95	>100	0.22	100.00	19.95	>100
Renal cancer																		
786-0	1.35	7.04	1.87	6.58	2.02	8.57	1.59	6.32	----	>100	1.77	6.19	1.78	7.20	0.13	51.64	0.79	>100
A498	----	----	5.73	44.9	5.87	46.5	----	----	100	>100	----	----	----	----	0.10	1.90	0.40	>100
ACHN	1.70	5.54	3.81	57.2	4.96	72.1	1.68	5.85	----	>100	1.60	5.43	1.33	5.16	0.08	100.00	0.32	>100
CAKI-1	1.87	5.72	4.30	51.0	4.38	86.2	1.71	5.62	100	>100	2.16	7.07	2.08	9.91	0.95	100.00	0.08	>100
RXF 393	1.80	6.12	3.31	38.3	2.81	41.1	1.50	5.63	----	>100	1.66	6.36	1.80	6.22	0.10	4.69	2.51	>100
SN12C	2.21	1.91	2.41	28.5	3.67	70.9	1.89	>100	----	----	1.91	9.11	1.95	>100	0.07	72.44	0.50	>100
TK-10	1.78	5.77	5.45	44.4	12.3	82.5	2.29	19.1	100	>100	2.51	1.53	2.44	20.4	0.38	89.95	----	----
UO-31	1.53	6.74	3.48	43.7	4.28	48.0	1.47	5.28	----	>100	1.59	5.42	1.34	5.21	0.49	26.18	1.26	>100
Prostate cancer																		
PC-3	1.79	8.33	2.38	43.2	2.91	73.6	1.83	35.9	----	>100	1.89	14.2	1.91	>100	0.32	87.10	1.58	>100
DU-145	1.47	5.28	3.36	33.1	3.52	36.3	1.69	7.23	----	>100	1.79	8.59	1.87	20.2	0.11	100.00	2.51	>100
Breast cancer																		
MCF7	0.31	29.2	2.11	>100	0.92	48.1	0.39	8.08	0.36	>100	1.88	32.9	0.42	63.7	0.04	64.12	0.40	>100
MDA-MB-231/ATCC	1.84	6.18	2.87	53.9	2.64	86.5	1.92	7.46	3.71	>100	2.51	31.6	2.93	>100	0.51	34.75	0.08	>100
HS 578T	3.01	>100	3.14	>100	4.14	>100	3.81	1.00	100	>100	3.18	>100	3.79	>100	0.33	85.70	6.31	>100
BT-549	0.70	5.49	2.25	23.3	3.29	43.5	1.37	5.16	2.03	>100	1.76	10.6	1.69	18.4	0.23	21.33	10.00	>100
T-47D	2.28	>100	3.33	>100	3.46	>100	2.63	1.00	----	>100	1.85	42.3	2.02	>100	0.06	85.70	10.00	>100
MDA-MB-468	1.64	8.62	2.32	>100	2.35	36.0	1.37	2.21	----	>100	1.46	16.0	1.65	49.3	0.05	2.52	7.94	>100

Abbreviation: SRB, sulforhodamine B.

^aData are obtained from NCI's in vitro disease-oriented human cancer cell lines screen in μM .

^b GI_{50} is the drug concentration resulting in a 50% reduction in the net protein increase (as measured by SRB staining) in control cells during the drug incubation, determined at five concentration levels (100, 10, 1.0, 0.1, and 0.01 μM).

^c LC_{50} is a parameter of cytotoxicity that reflects the molar concentration needed to kill 50% of the cells.

^dThe values of activity against human cancer cell lines displayed by adriamycin/doxorubicin correspond to that reported by NCI at highest concentration of 100 μM . For more details, please visit <https://dtp.cancer.gov/dtpstandard/cancerscreeningdata/index.jsp>. The most outstanding GI_{50} values are highlighted in red color.

elemental analyzer, and the values are within $\pm 0.4\%$ of the theoretical values. Thin-layer chromatography (TLC) analyses were performed on silica gel aluminum plates (Merck 60 F₂₅₄) and spots were visualized with ultraviolet irradiation.

The InChI codes of the investigated compounds, together with some biological activity data, are provided as Supporting Information.

4.1.2 | General procedure for the synthesis of symmetrical bis-quinolinyl-chalcones **14a-k**

A mixture of substituted 3-formylquinolines (**10-12**) (1 mmol), acetone (0.5 mmol), and 20% aq. KOH (0.5 ml) in MeOH (10 ml)

was stirred at ambient temperature for 11–13 h. Then, the reaction mixture was neutralized with acid acetic. The resulting precipitate was collected by filtration under vacuum and washed with methanol (2 \times 3 ml), followed by water (2 \times 3 ml), and then dried and purified by recrystallization or by column chromatography on silica gel.

3,3'-((1E,4E)-3-Oxopenta-1,4-diene-1,5-diyl)bis(6-methylquinolin-2(1H)-one) **14a**

Yellow solid, m.p. $>300^\circ\text{C}$. FTIR (ATR): $\nu = 3154$ (NH), [1661, 1659] (C=O) cm^{-1} . ^1H NMR (400 MHz, DMSO-*d*₆) $\delta = 2.30$ (s, 6H, CH₃ \times 2), 7.27 (d, $J = 7.9$ Hz, 2H), 7.42 (d, $J = 8.1$ Hz, 2H), 7.52 (s, 2H), 7.74 (d, $J = 15.9$ Hz, 2H, =CH \times 2), 7.81 (d, $J = 15.9$ Hz, 2H, =CH \times 2), 8.44 (s, 2H), 12.03 (s, 2H, NH). ^{13}C NMR (101 MHz, DMSO-*d*₆) $\delta = 27.9$,

TABLE 5 Binding affinities for the selected quinolinyl-chalcones **14g** and **17b–e,n,o** compared with known chemotherapeutic drugs

Protein (treatment)	Binding energy (kcal/mol) ^a							
	Known inhibitors (PDB code) ^b	14g	17b	17c	17d	17e	17n	17o
HER2 (colorectal cancer [CRC] breast cancer)	SYR127063 (3PP0)	-11.4						
	Lapatinib	-10.7	-8.7	-10.0	-10.5	-10.2	-10.9	-9.5 -10.3
	Afatinib	-9.4						
HER1 (CRC, breast cancer)	Rociletinib (5XDL)	-						
	Gefitinib (4WKQ)	-7.3	-8.1	-7.8	-8.1	-7.7	-8.2	-7.6 -8.3
	Erlotinib (1M17)	-6.3						
VEGFR2 (CRC)	Axitinib (4AG8)	-9.2						
	Sorafenib (3WZE)	-10.8	-9.1	-10.8	-	-10.1	-11.4	-9.5 -10.4
	Lenvatinib (3WZD)	-8.9						
	Regorafenib	-10.8						
BRAF (melanoma)	Vemurafenib (3OG7)	-9.3						
	Dabrafenib (4XV2)	-12.9	-9.0	-10.1	-	-9.7	-	- -9.7
Proteasome (leukemia, CRC)	PRD_001075 (3SDK)	-						
	Bortezomib (5LF3)	-7.8						
	Ixazomib (5LF7)	-7.8	-8.5	-9.3	-	-9.3	-9.5	-8.9 -9.6
Bcl-2 (Leukemia)	Carfilzomib (4R67)	-8.5						
	Navitoclax (4LVT)	-8.3						
	Venetoclax (6O0K)	-8.2	-8.5	-7.9	-	-8.0	-8.0	- -9.7
hTS (CRC)	dUMP (5X5D)	-						
	Raltitrexed (5X5Q)	-8.0	-8.1	-9.2	-	-8.6	-8.9	-8.5 -8.8
	5FdUMP (6QXG)	-7.7						

^aBest binding energies for known inhibitors, and for the studied compounds that yielded similar or better results than the reference inhibitors for each protein, are shown in bold numbers.

^bPDB codes for the complexes of the known inhibitors with the considered proteins (PDB codes shown in bold are those corresponding to each protein structure employed in the docking calculations).

117.4, 120.5, 126.5, 127.3, 127.81, 130.4, 131.9, 137.9, 138.0, 140.1, 160.9, 198.8 ppm. Electrospray ionization mass spectroscopy (EI MS) (70 eV): *m/z* (%): 396 (M^+ , 1), 368 (11), 313 (10), 236 (28), 57 (100). Anal. calcd. for $C_{25}H_{20}N_2O_3$: C, 75.74; H, 5.09; N, 7.07. Found: C, 75.48; H, 4.88; N, 7.23.

3,3'-((1E,4E)-3-Oxopenta-1,4-diene-1,5-diyl)bis(7-chloroquinolin-2(1H)-one) 14b

Yellow solid, m.p. >300°C. FTIR (ATR): $\nu = 3151$ (NH), [1662, 1654] (C=O) cm^{-1} . 1H NMR (400 MHz, DMSO- d_6) $\delta = 7.21$ (dd, $J = 8.4, 2.0$ Hz, 2H), 7.41 (d, $J = 2.0$ Hz, 2H), 7.68 (s, 4H, =CH $\times 4$), 7.72 (d, $J = 8.5$ Hz, 2H), 8.35 (s, 2H), 11.65 (s, 2H, NH). ^{13}C NMR (101 MHz, DMSO- d_6) $\delta = 113.8, 117.4, 121.7, 126.1, 128.0, 129.6, 135.5, 136.5, 139.2, 139.2, 159.9, 188.6$ ppm. EI MS (70 eV): *m/z* (%): 256 (5), 236 (3), 149 (12), 137 (12), 97 (23), 69 (100). Anal. calcd. for $C_{23}H_{14}Cl_2N_2O_3$: C, 63.18; H, 3.23; N, 6.41. Found: C, 63.29; H, 3.10; N, 6.60.

3,3'-((1E,4E)-3-Oxopenta-1,4-diene-1,5-diyl)bis(8-methylquinolin-2(1H)-one) 14c

Yellow solid, m.p. >300°C. FTIR (ATR): $\nu = 3161$ (NH), [1671, 1649] (C=O) cm^{-1} . 1H NMR (400 MHz, DMSO- d_6) $\delta = 2.16$ (s, 6H, $CH_3 \times 2$), 7.12 (t, $J = 7.5$ Hz, 2H), 7.16 (d, $J = 16.3$ Hz, 2H, =CH $\times 2$), 7.35 (d, $J = 7.2$ Hz, 2H), 7.43 (d, $J = 16.6$ Hz, 2H, =CH $\times 2$), 7.53 (d, $J = 7.8$ Hz, 2H), 8.17 (s, 2H, NH). ^{13}C NMR (101 MHz, DMSO- d_6) $\delta = 12.4, 119.9, 122.5, 123.7, 126.7, 127.7, 129.0, 132.2, 132.3, 136.9, 137.6, 161.8, 179.2$ ppm. EI MS (70 eV): *m/z* (%): 396 (M^+ , 1), 368 (15), 236 (27), 57 (100). Anal. calcd. for $C_{25}H_{20}N_2O_3$: C, 75.74; H, 5.09; N, 7.07. Found: C, 75.86; H, 5.20; N, 6.89.

3,3'-((1E,4E)-3-Oxopenta-1,4-diene-1,5-diyl)bis(6-chloroquinolin-2(1H)-one) 14d

Yellow solid, m.p. >300°C. FTIR (ATR): $\nu = 3154$ (NH), 1658 ($2 \times C=O$) cm^{-1} . 1H NMR (400 MHz, DMSO- d_6) $\delta = 7.38$ (d, $J = 8.8$ Hz, 2H), 7.62 (dd, $J = 8.8, 2.3$ Hz, 2H), 7.72 (d, $J = 15.9$ Hz, 2H, =CH $\times 2$), 7.80 (d, $J = 15.9$ Hz,

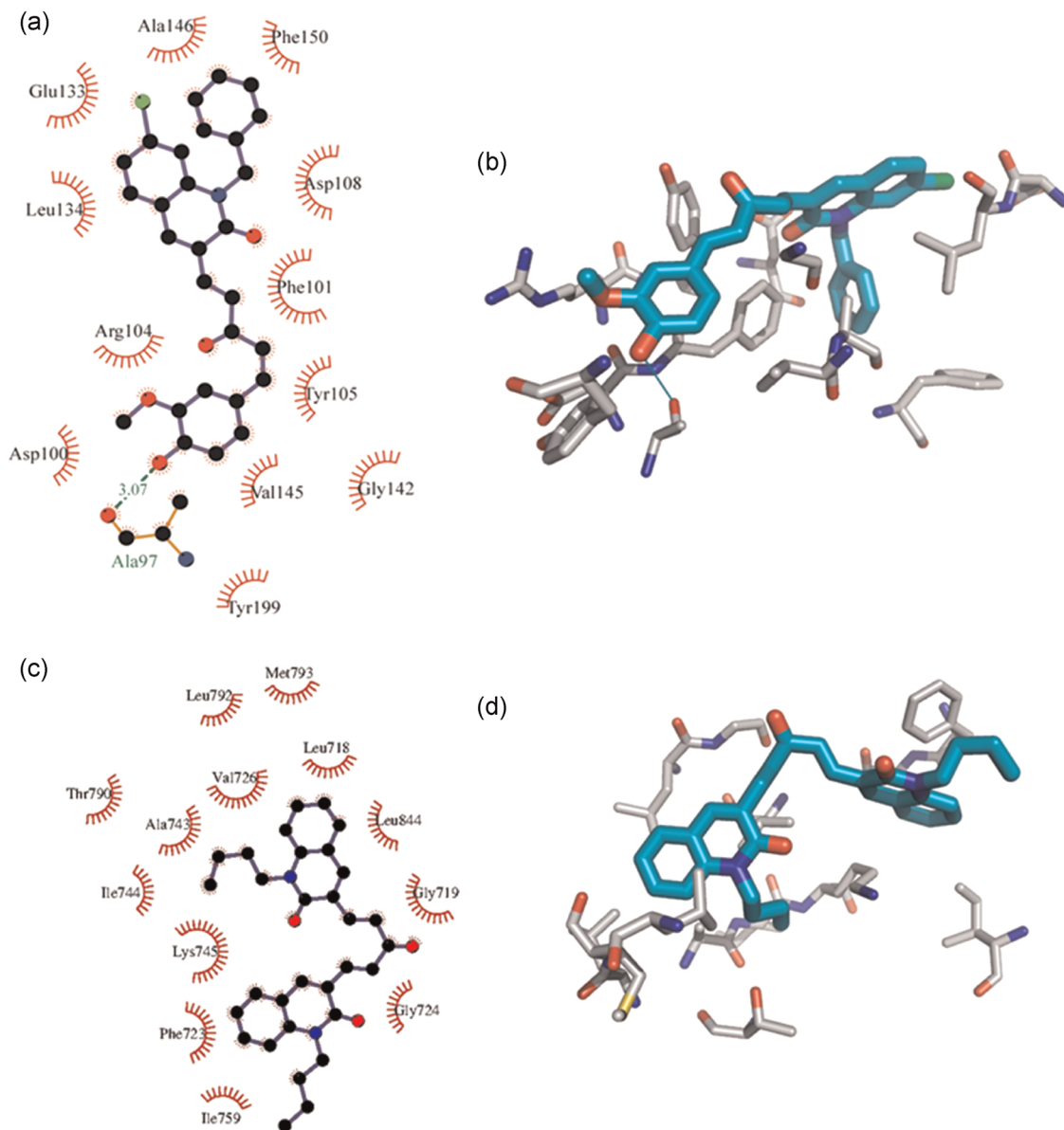


FIGURE 3 (a) Two-dimensional (2D) representation of the most favorable binding pose of ligand **17o** in the active site of Bcl-2. Hydrophobic interactions between the ligand atoms and the protein residues are depicted as red radial lines, and hydrogen bonds as green dotted lines. (b) Three-dimensional (3D) representation of the most favorable binding mode of ligand **17o** in the active site of Bcl-2. Hydrogen-bond interactions are shown as green lines. (c) 2D representation of the most favorable binding pose of ligand **14g** in the active site of HER1. Hydrophobic interactions between the ligand atoms and the protein residues are depicted as red radial lines. (d) 3D representation of the most favorable binding mode of ligand **14g** in the active site of HER1

2H, =CH × 2), 7.83 (d, $J = 2.2$ Hz, 2H), 8.49 (s, 2H, NH). Compound **14d** is barely soluble in CDCl_3 and DMSO, thus, made the registration of a high-resolution ^{13}C NMR spectrum impossible. EI MS (70 eV): m/z (%): 396 (M^+ , 5), 313 (10), 236 (24), 57 (100). Anal. calcd. for $\text{C}_{23}\text{H}_{14}\text{Cl}_2\text{N}_2\text{O}_3$: C, 63.18; H, 3.23; N, 6.41. Found: C, 63.01; H, 3.05; N, 6.60.

3,3'-((1E,4E)-3-Oxopenta-1,4-diene-1,5-diyl)bis(6-bromoquinolin-2(1H)-one) **14e**

Yellow solid, m.p. $>300^\circ\text{C}$. FTIR (ATR): $\nu = 3135$ (NH), [1671, 1668] ($\text{C}=\text{O}$) cm^{-1} . ^1H NMR (400 MHz, $\text{DMSO}-d_6$) $\delta = 6.92$ (dd, $J = 8.4, 1.8$ Hz, 2H), 7.00 (s, 2H), 7.35 (d, $J = 15.9$ Hz, 2H, =CH × 2), 7.40 (d,

$J = 8.4$ Hz, 2H), 7.42 (d, $J = 15.9$ Hz, 2H, =CH × 2), 8.16 (s, 2H), 11.81 (s, 2H, NH). Compound **14e** is barely soluble in CDCl_3 and DMSO, which thus made the registration of a high-resolution ^{13}C NMR spectrum impossible. EI MS (70 eV): m/z (%): 249/247 (98/100). Anal. calcd. for $\text{C}_{23}\text{H}_{14}\text{Br}_2\text{N}_2\text{O}_3$: C, 52.50; H, 2.68; N, 5.32. Found: C, 52.67; H, 2.51; N, 5.19.

3,3'-((1E,4E)-3-Oxopenta-1,4-diene-1,5-diyl)bis(6-methoxyquinolin-2(1H)-one) **14f**

Yellow solid, m.p. $>300^\circ\text{C}$. FTIR (ATR): $\nu = 3161$ (NH), 1657 ($2 \times \text{C}=\text{O}$) cm^{-1} . ^1H NMR (400 MHz, $\text{DMSO}-d_6$) $\delta = 3.92$ (s, 6H, OCH_3),

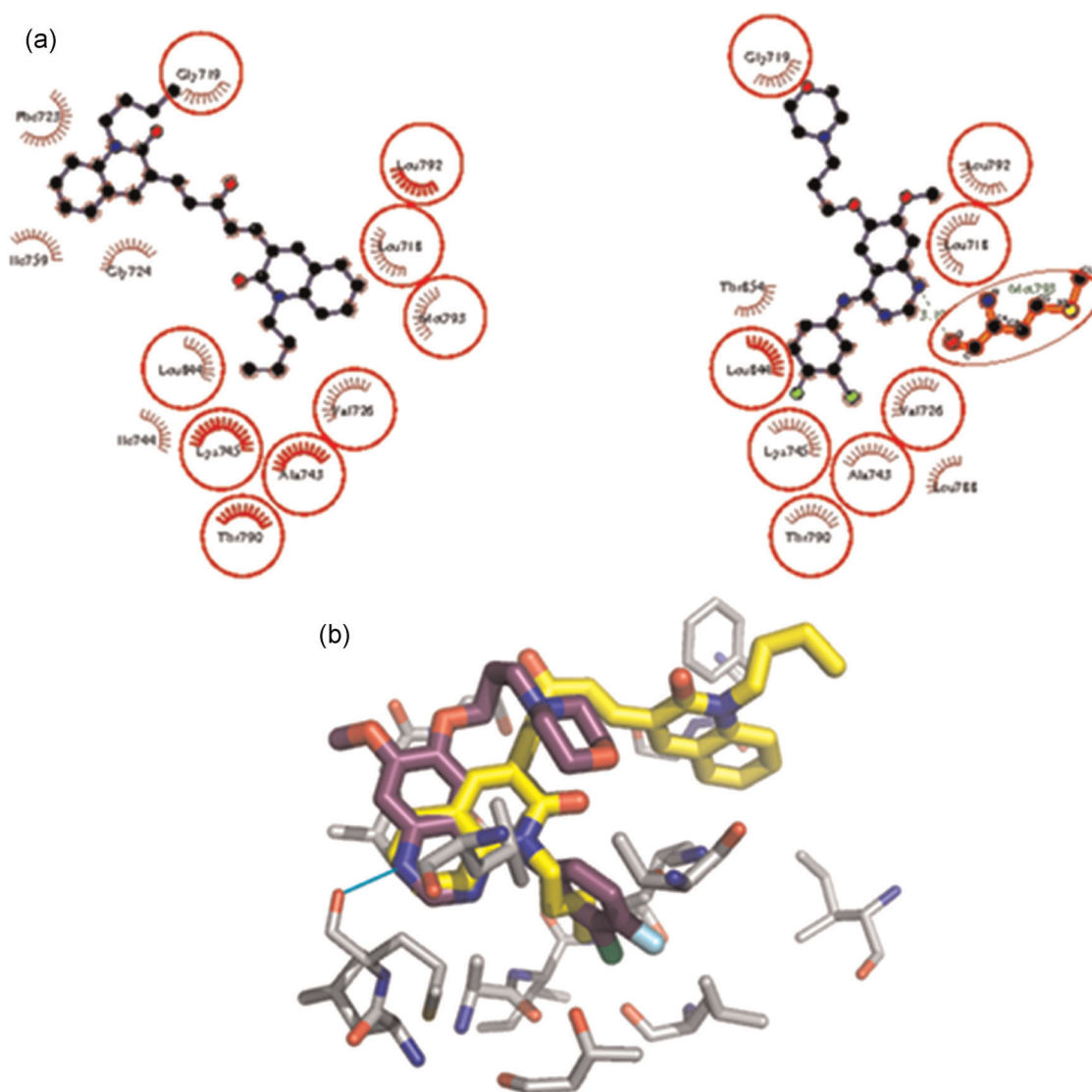


FIGURE 4 (a) Two-dimensional representations of the most favorable binding pose of ligand **14g** (left) and of gefitinib (right) in the active site of HER1. Red circles indicate residues involved in interactions with both ligands. (b) Superimposed three-dimensional representations of the most favorable binding modes for **14g** (in yellow) and gefitinib (in purple) in the active site of HER1. Hydrogen-bond interactions are shown as cyan lines

7.26 (d, $J = 16.6$ Hz, 2H, =CH $\times 2$), 7.35 (d, $J = 9.0$ Hz, 2H), 7.46 (d, $J = 16.6$ Hz, 2H, =CH $\times 2$), 7.57 (d, $J = 9.1$ Hz, 2H), 8.23 (s, 2H). ^{13}C NMR (101 MHz, DMSO- d_6) $\delta = 60.7, 115.8, 121.3, 124.7, 125.9, 132.4, 132.8, 134.0, 137.1, 138.9, 140.0, 159.6, 184.0$ ppm. EI MS (70 eV): m/z (%): 428 (M^+ , 12), 200 (100), 236 (22). Anal. calcd. for $\text{C}_{25}\text{H}_{20}\text{N}_2\text{O}_5$: C, 70.09; H, 4.71; N, 6.54. Found: C, 69.90; H, 4.88; N, 6.44.

3,3'-((1E,4E)-3-Oxopenta-1,4-diene-1,5-diyI)bis(1-butylquinolin-2(1H)-one) **14g**

Yellow solid, m.p. 180–181°C. FTIR (ATR): $\nu = [1668, 1659]$ (C=O) cm^{-1} . ^1H NMR (400 MHz, CDCl_3) $\delta = 1.06$ (t, $J = 7.3$ Hz, 6H, $\text{CH}_3 \times 2$), 1.63–1.42 (m, 4H, $\text{CH}_2 \times 2$), 1.85–1.71 (m, 4H, $\text{CH}_2 \times 2$), 4.42–4.23 (m, 4H, $\text{NCH}_2 \times 2$), 7.28 (t, $J = 7.5$ Hz, 2H), 7.29 (d, $J = 6.1$ Hz, 2H), 7.39 (t, $J = 8.6$ Hz, 2H), 7.62 (d, $J = 7.6$ Hz, 2H), 7.66

(d, $J = 8.3$ Hz, 2H), 7.81 (d, $J = 15.9$ Hz, 2H, =CH $\times 2$), 7.90 (d, $J = 15.9$ Hz, 2H, =CH $\times 2$), 8.01 (s, 2H), ^{13}C NMR (101 MHz, CDCl_3) $\delta = 13.9, 20.4, 29.6, 42.7, 114.2, 120.5, 122.3, 126.4, 129.0, 129.9, 131.7, 138.4, 139.3, 139.9, 160.7, 190.3$ ppm. EI MS (70 eV): m/z (%): 480 (M^+ , 10), 381 (41), 204 (47), 194 (100), 57 (32). Anal. calcd. for $\text{C}_{31}\text{H}_{32}\text{N}_2\text{O}_3$: C, 77.47; H, 6.71; N, 5.83. Found: C, 77.60; H, 6.83; N, 5.71.

3,3'-((1E,4E)-3-Oxopenta-1,4-diene-1,5-diyI)bis(1-butyl-6-methoxyquinolin-2(1H)-one) **14h**

Yellow solid, m.p. 174–175°C; FTIR (ATR) $\nu = [1650, 1603]$ (C=O) cm^{-1} . ^1H NMR (400 MHz, CDCl_3) $\delta = 1.09$ (t, $J = 7.4$ Hz, 6H, $\text{CH}_3 \times 2$), 1.57–1.66 (m, 4H, $\text{CH}_2 \times 2$), 1.90–1.97 (m, 4H, $\text{CH}_2 \times 2$), 3.93 (s, 6H, $\text{OCH}_3 \times 2$), 4.58 (t, $J = 6.5$ Hz, 4H, $\text{NCH}_2 \times 2$), 7.02 (d, $J = 16.3$ Hz, 2H,

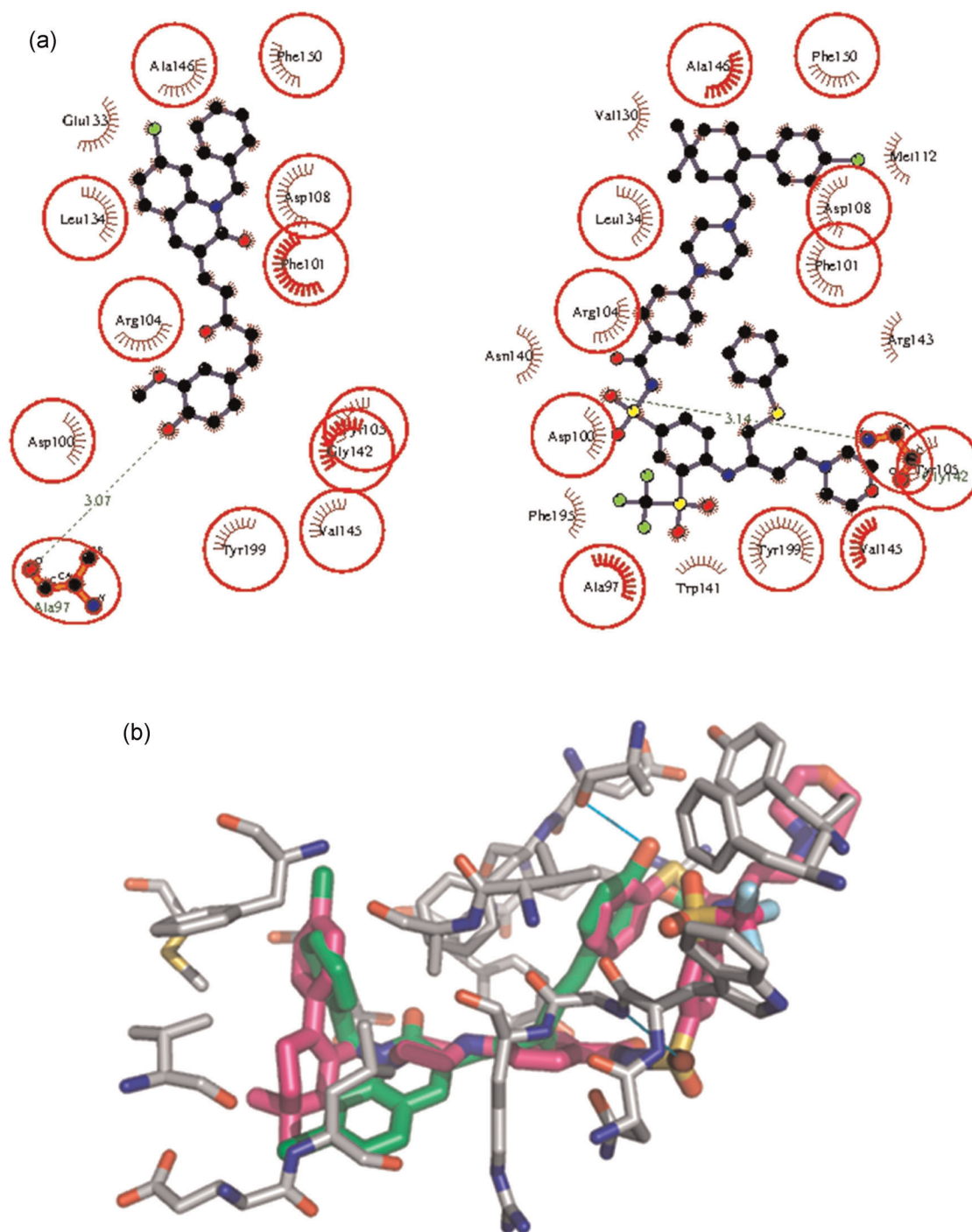


FIGURE 5 (a) Two-dimensional representations of the most favorable binding pose of ligand **17o** (left) and of navitoclax (right) in the active site of Bcl-2. Red circles indicate residues involved in interactions with both ligands. (b) Superimposed three-dimensional representations of the most favorable binding modes for **17o** (in green) and navitoclax (in magenta) in the active site of Bcl-2. Hydrogen-bond interactions are shown as cyan lines

=CH × 2), 7.31 (d, $J = 10.7$ Hz, 2H), 7.77 (d, $J = 9.0$ Hz, 2H), 7.89 (d, $J = 15.7$ Hz, 2H, =CH × 2), 8.08 (s, 2H), ^{13}C NMR (400 MHz, CDCl_3) $\delta = 14.0, 19.6, 31.1, 55.6, 66.5, 106.3, 120.3, 122.5, 125.49, 127.23, 128.21, 135.5, 137.6, 142.2, 156.4, 158.7, 183.5$ ppm. EI MS (70 eV): m/z (%): 540 (M^+ , 6), 256 (100), 200 (51). Anal. calcd. for $\text{C}_{33}\text{H}_{36}\text{N}_2\text{O}_5$: C, 73.31; H, 6.71; N, 5.18. Found: C, 73.50; H, 6.64; N, 5.06.

3,3'-((1E,4E)-3-Oxopenta-1,4-diene-1,5-diyI)bis(1-butyl-6-chloroquinolin-2(1H)-one) **14i**

Yellow solid, m.p. 162–163°C. FTIR (ATR): $\nu = [1653, 1642]$ ($\text{C}=\text{O}$) cm^{-1} . ^1H NMR (400 MHz, CDCl_3) $\delta = 1.07$ (t, $J = 7.2$ Hz, 6H, $\text{CH}_3 \times 2$), 1.52–1.58 (m, 4H, $\text{CH}_2 \times 2$), 1.75–1.82 (m, 4H, $\text{CH}_2 \times 2$), 4.32 (t, $J = 7.4$ Hz, 4H, $\text{NCH}_2 \times 2$), 7.25 (d, $J = 8.2$ Hz, 2H), 7.37 (s, 2H), 7.49 (d, $J = 15.7$ Hz, 2H, =CH × 2), 7.59 (d, $J = 8.3$ Hz, 2H), 7.70 (d, $J = 15.7$ Hz,

2H, =CH × 2), 7.88 (s, 2H). ¹³C NMR (400 MHz, CDCl₃) δ = 14.0, 19.5, 31.0, 66.8, 120.5, 123.3, 125.4, 126.2, 127.5, 129.0, 134.9, 136.5, 137.9, 147.1, 160.6, 183.3 ppm. EI MS (70 eV): *m/z* (%): 550/548 (M⁺, 18/57), 260 (100), 204 (43). Anal. calcd. for C₃₁H₃₀Cl₂N₂O₃: C, 67.76; H, 5.50; N, 5.10. Found: C, 67.85; H, 5.42; N, 5.23.

(1E,4E)-1,5-Bis(2-butoxyquinolin-3-yl)penta-1,4-dien-3-one 14j

Yellow solid, m.p. 157–158°C. FTIR (ATR): ν = 1666 (C=O) cm⁻¹. ¹H NMR (400 MHz, CDCl₃) δ = 1.08 (t, *J* = 7.4 Hz, 6H, CH₃ × 2), 1.71–1.56 (m, 4H, CH₂ × 2), 2.04–1.91 (m, 4H, CH₂ × 2), 4.66 (t, *J* = 6.7 Hz, 4H, NCH₂ × 2), 7.42 (d, *J* = 7.2 Hz, 2H), 7.47 (d, *J* = 16.2 Hz, 2H, =CH × 2), 7.69 (t, *J* = 7.6 Hz, 2H), 7.79 (d, *J* = 8.0 Hz, 2H), 7.88 (d, *J* = 8.4 Hz, 2H), 8.03 (d, *J* = 16.0 Hz, 2H, =CH × 2), 8.29 (s, 2H). ¹³C NMR (101 MHz, CDCl₃) δ = 14.0, 31.1, 19.6, 66.6, 120.3, 124.6, 125.0, 127.0, 128.0, 128.5, 130.8, 138.0, 138.9, 147.9, 160.1, 189.5 ppm. EI MS (70 eV): *m/z* (%): 381 (M⁺, 56), 204 (25), 179 (24). Anal. calcd. for C₃₁H₃₂N₂O₃: C, 77.47; H, 6.71; N, 5.83. Found: C, 77.60; H, 6.50; N, 5.93.

(1E,4E)-1,5-Bis(2-butoxy-8-methylquinolin-3-yl)penta-1,4-dien-3-one 14k

Yellow solid, m.p. 150–151°C. FTIR (ATR): ν = 1665 (C=O) cm⁻¹. ¹H NMR (400 MHz, CDCl₃) δ = 1.08 (t, *J* = 7.4 Hz, 6H, CH₃ × 2), 1.70–1.57 (m, 4H, CH₂ × 2), 2.05–1.92 (m, 4H, CH₂ × 2), 2.73 (s, 6H, CH₃ × 2), 4.67 (t, *J* = 6.7 Hz, 4H, OCH₂ × 2), 7.33 (t, *J* = 7.6 Hz, 2H), 7.50 (d, *J* = 16.0 Hz, 2H, =CH × 2), 7.55 (d, *J* = 6.9 Hz, 2H), 7.64 (d, *J* = 8.0 Hz, 2H), 8.03 (d, *J* = 16.0 Hz, 2H, =CH × 2), 8.26 (s, 2H). ¹³C NMR (101 MHz, CDCl₃) δ = 14.0, 17.7, 19.6, 31.0, 66.2, 119.7, 124.2, 124.8, 125.9, 128.3, 130.9, 135.2, 138.2, 139.2, 145.8, 159.0, 189.7 ppm. EI MS (70 eV): *m/z* (%): 508 (M⁺, 1), 503 (28), 432 (27), 306 (160), 43 (100). Anal. calcd. for C₃₃H₃₆N₂O₃: C, 77.92; H, 7.13; N, 5.51. Found: C, 78.10; H, 7.01; N, 5.70.

4.1.3 | General procedure for the synthesis of unsymmetrical quinolinyl-bis-chalcones 17a–w

A mixture of the arylidene acetones 16a–d (0.05 mmol), 3-formylquinolines 10–12 (0.05 mmol), and 20% aq. KOH (0.5 ml) in MeOH (10 ml) was stirred at ambient temperature for 4–20 h until the starting reagents were not detected by TLC. Then, the reaction mixture was neutralized with acetic acid. The resulting precipitate was collected by filtration under vacuum and washed with methanol (2 × 3 ml), followed by water (2 × 3 ml), and then dried and purified by recrystallization or by column chromatography on silica gel.

3-((1E,4E)-5-(4-Hydroxy-3-methoxyphenyl)-3-oxopenta-1,4-dien-1-yl)quinolin-2(1H)-one 17a

Yellow solid, m.p. 259–260°C. FTIR (ATR): ν = [3264, 3238] (OH, NH), [1669, 1666] (C=O) cm⁻¹. ¹H NMR (400 MHz, DMSO-*d*₆) δ = 3.88 (s, 1H, OCH₃), 6.86 (d, *J* = 8.1 Hz, 1H), 7.17 (d, *J* = 15.9 Hz, 1H, =CH), 7.23 (d, *J* = 7.7 Hz, 1H), 7.24 (t, *J* = 7.6 Hz, 1H), 7.36 (d,

J = 8.2 Hz, 1H), 7.43 (s, 1H), 7.57 (t, *J* = 7.7 Hz, 1H), 7.67 (d, *J* = 15.9 Hz, 1H, =CH), 7.74 (d, *J* = 8.2 Hz), 7.74 (d, *J* = 15.9 Hz, 1H, =CH), 7.82 (d, *J* = 15.9 Hz, 1H, =CH), 8.46 (s, 1H), 12.08 (s, 1H, NH), OH was not observed. ¹³C NMR (101 MHz, DMSO-*d*₆) δ = 56.2, 111.9, 115.6, 116.2, 119.6, 122.8, 123.7, 124.2, 126.7, 126.7, 128.6, 129.1, 132.1, 137.7, 139.3, 141.6, 144.0, 148.5, 150.2, 161.4, 189.0 ppm. EI MS (70 eV): *m/z* (%): 347 (M⁺, 24), 170 (100). Anal. calcd. for C₂₁H₁₇NO₄: C, 72.61; H, 4.93; N, 4.03. Found: C, 72.73; H, 5.05; N, 3.86.

3-((1E,4E)-5-(4-Methoxyphenyl)-3-oxopenta-1,4-dien-1-yl)quinolin-2(1H)-one 17b

Yellow solid, m.p. 259–260°C. FTIR (ATR): ν = 3240 (NH), [1681, 1679] (C=O) cm⁻¹. ¹H NMR (400 MHz, DMSO-*d*₆) δ = 3.83 (s, 3H, OCH₃), 7.03 (d, *J* = 8.6 Hz, 2H), 7.20 (d, *J* = 16.0 Hz, 1H, =CH), 7.25 (t, *J* = 7.5 Hz, 1H), 7.37 (d, *J* = 8.2 Hz, 1H), 7.58 (t, *J* = 7.5 Hz, 1H), 7.71 (d, *J* = 16.0 Hz, 1H, =CH), 7.74 (d, *J* = 6.6 Hz, 1H), 7.86–7.75 (m, 4H, =CH, Ar-H), 8.47 (s, 1H, NH). ¹³C NMR (101 MHz, DMSO-*d*₆) δ = 55.9, 115.0, 115.6, 119.6, 122.8, 124.2, 126.6, 127.7, 128.5, 129.1, 131.0, 132.2, 138.0, 139.5, 141.6, 143.1, 161.4, 161.8, 189.1 ppm. EI MS (70 eV): *m/z* (%): 331 (M⁺, 41), 303 (19), 170 (100), 57 (24). Anal. calcd. for C₂₁H₁₇NO₃: C, 76.12; H, 5.17; N, 4.23. Found: C, 76.00; H, 5.30; N, 4.42.

3-((1E,4E)-5-(4-Chlorophenyl)-3-oxopenta-1,4-dien-1-yl)quinolin-2(1H)-one 17c

Yellow solid, m.p. 259–260°C. FTIR (ATR): ν = 3248 (NH), [1663, 1658] (C=O) cm⁻¹. ¹H NMR (400 MHz, DMSO-*d*₆) δ = 7.25 (t, *J* = 7.5 Hz, 1H), 7.37 (d, *J* = 7.7 Hz, 1H), 7.39 (d, *J* = 16.0 Hz, 1H, =CH), 7.53 (d, *J* = 8.3 Hz, 2H), 7.58 (t, *J* = 7.6 Hz, 1H), 7.71 (d, *J* = 16.0 Hz, 1H, =CH), 7.74 (d, *J* = 7.3 Hz, 1H), 7.81 (s, 2H, =CH × 2), 7.86 (d, *J* = 8.4 Hz, 2H), 8.47 (s, 1H), NH was not observed. ¹³C NMR (101 MHz, DMSO-*d*₆) δ = 115.7, 119.6, 122.8, 126.5, 127.0, 128.5, 129.2, 129.5, 130.8, 132.3, 134.2, 135.5, 138.8, 139.5, 141.6, 142.0, 161.4, 189.3 ppm. EI MS (70 eV): *m/z* (%): 337/335 (M⁺, 12/37), 170 (100). Anal. calcd. for C₂₀H₁₄ClNO₂: C, 71.54; H, 4.20; N, 4.17. Found: C, 71.66; H, 4.45; N, 4.01.

3-((1E,4E)-5-(4-Hydroxy-3-methoxyphenyl)-3-oxopenta-1,4-dien-1-yl)-6-methoxyquinolin-2(1H)-one 17d

Yellow solid, m.p. 259–260°C. FTIR (ATR): ν = [3435, 3176] (OH, NH), [1662, 1639] (C=O) cm⁻¹. ¹H NMR (400 MHz, DMSO-*d*₆) δ = 3.82 (s, 3H, OCH₃), 3.88 (s, 3H, OCH₃), 6.85 (d, *J* = 8.1 Hz, 1H), 7.16 (d, *J* = 15.9 Hz, 1H, =CH), 7.28–7.20 (m, 3H), 7.31 (d, *J* = 9.7 Hz, 1H), 7.43 (s, 1H), 7.67 (d, *J* = 15.9 Hz, 1H, =CH), 7.72 (d, *J* = 15.9 Hz, 1H, =CH), 7.83 (d, *J* = 15.9 Hz, 1H, =CH), 8.39 (s, 1H), 11.99 (s, 1H, NH). ¹³C NMR (101 MHz, DMSO-*d*₆) δ = 56.0, 56.2, 109.8, 111.9, 116.2, 116.9, 120.1, 121.8, 123.7, 124.2, 126.7, 126.9, 128.6, 134.1, 137.8, 141.2, 144.0, 148.5, 150.2, 154.9, 160.9, 189.0 ppm. EI MS (70 eV): *m/z* (%): 377 (M⁺, 32), 262 (14), 200 (100), 157 (57). Anal. calcd. for C₂₂H₁₉NO₅: C, 70.02; H, 5.07; N, 3.71. Found: C, 70.20; H, 5.16; N, 3.50.

3-((1E,4E)-5-(4-Chlorophenyl)-3-oxopenta-1,4-dien-1-yl)-8-methylquinolin-2(1H)-one 17e

Yellow solid, m.p. 256–257°C. FTIR (ATR): $\nu = 3150$ (NH), [1672, 1665] (C=O) cm^{-1} . ^1H NMR (400 MHz, DMSO- d_6) $\delta = 2.34$ (s, 3H, CH₃), 7.24 (d, $J = 8.4$ Hz, 1H), 7.36 (d, $J = 8.3$ Hz, 1H), 7.37 (d, $J = 16.0$ Hz, 1H, =CH), 7.46 (s, 1H), 7.50 (d, $J = 8.5$ Hz, 2H), 7.67 (d, $J = 16.0$ Hz, 1H, =CH), 7.78 (s, 2H, =CH $\times 2$), 7.83 (d, $J = 8.5$ Hz, 2H), 8.33 (s, 1H). ^{13}C NMR (101 MHz, DMSO- d_6) $\delta = 20.3, 115.4, 119.1, 125.7, 126.4, 127.8, 127.9, 129.0, 130.2, 131.0, 133.1, 133.7, 134.9, 137.7, 138.8, 140.9, 141.3, 161.1, 188.8$ ppm. EI MS (70 eV): m/z (%): 351/349 (M⁺, 16/58), 184 (100), 157 (35). Anal. calcd for C₂₁H₁₆ClNO₂: C, 72.10; H, 4.61; N, 4.00. Found: C, 69.96; H, 4.82; N, 4.21.

6-Chloro-3-((1E,4E)-5-(4-chlorophenyl)-3-oxopenta-1,4-dien-1-yl)quinolin-2(1H)-one 17f

Yellow solid, m.p. >300°C. FTIR (ATR): $\nu = 3248$ (NH), [1663, 1658] (C=O) cm^{-1} . ^1H NMR (400 MHz, DMSO- d_6) $\delta = 7.22$ (d, $J = 16.0$ Hz, 1H, =CH), 7.38 (d, $J = 8.8$ Hz, 1H), 7.47 (d, $J = 8.5$ Hz, 2H), 7.53 (dd, $J = 8.8, 2.3$ Hz, 1H), 7.65 (d, $J = 16.0$ Hz, 1H, =CH), 7.68–7.77 (m, 5H, =CH, Ar-H), 8.30 (s, 1H). ^{13}C NMR (101 MHz, DMSO- d_6) $\delta = 116.3, 119.6, 125.6, 126.2, 126.6, 127.1, 128.2, 128.3, 129.3, 130.5, 133.2, 134.4, 136.6, 137.1, 138.6, 140.3, 159.8, 188.2$ ppm. EI MS (70 eV): m/z (%): 206/204 (31/100). Anal. calcd. for C₂₀H₁₃Cl₂NO₂: C, 64.88; H, 3.54; N, 3.78. Found: C, 65.01; H, 3.71; N, 3.60.

3-((1E,4E)-5-(4-Methoxyphenyl)-3-oxopenta-1,4-dien-1-yl)-8-methylquinolin-2(1H)-one 17g

Yellow solid, m.p. 260–261°C. FTIR (ATR): $\nu = 3253$ (NH), [1668, 1657] (C=O) cm^{-1} . ^1H NMR (400 MHz, DMSO- d_6) $\delta = 2.48$ (s, 3H, CH₃), 3.84 (s, 3H, OCH₃), 7.01 (d, $J = 8.8$ Hz, 1H), 7.08 (d, $J = 15.9$ Hz, 1H, =CH), 7.13 (t, $J = 7.6$ Hz, 1H), 7.39 (d, $J = 7.3$ Hz, 1H), 7.55 (d, $J = 7.7$ Hz, 1H), 7.63 (d, $J = 16.3$ Hz, 1H, =CH), 7.67 (d, $J = 16.0$ Hz, 2H, =CH), 7.68 (d, $J = 8.8$ Hz, 2H), 7.74 (d, $J = 16.0$ Hz, 1H, =CH), 8.32 (s, 1H), 10.56 (s, 1H, NH). ^{13}C NMR (101 MHz, DMSO- d_6) $\delta = 15.8, 54.8, 114.1, 118.7, 121.3, 122.7, 123.5, 125.6, 126.0, 127.0, 127.8, 129.4, 132.0, 136.3, 136.8, 140.1, 141.6, 160.4, 160.9, 188.1$ ppm. EI MS (70 eV): m/z (%): 184 (100) 133 (23), 41 (31). Anal. calcd. for C₂₂H₁₉NO₃: C, 76.50; H, 5.54; N, 4.06. Found: C, 76.77; H, 5.30; N, 4.18.

3-((1E,4E)-5-(4-Chlorophenyl)-3-oxopenta-1,4-dien-1-yl)benzo[h]-quinolin-2(1H)-one 17h

Yellow solid, m.p. 270–271°C. FTIR (ATR): $\nu = 3231$ (NH), [1659, 1652] (C=O) cm^{-1} . ^1H NMR (400 MHz, DMSO- d_6) $\delta = 7.26$ (d, $J = 16.0$ Hz, 1H, =CH), 7.48 (d, $J = 8.5$ Hz, 2H), 7.71–7.61 (m, 4H), 7.68 (d, $J = 16.1$ Hz, 1H, =CH), 7.75 (d, $J = 16.1$ Hz, 1H, =CH), 7.76 (d, $J = 8.4$ Hz, 2H), 7.82 (d, $J = 16.1$ Hz, 1H, =CH), 7.99–7.94 (m, 1H), 8.46 (s, 1H), 8.89 (d, $J = 8.0$ Hz, 1H), 11.95 (s, 1H, NH). ^{13}C NMR (101 MHz, DMSO- d_6) $\delta = 111.4, 122.0, 122.1, 123.9, 124.6, 125.8, 126.3, 127.4, 127.7, 128.2, 129.3, 133.3 \times 2, 133.7, 133.8, 133.9, 134.3, 137.1, 140.0, 140.8, 160.5, 188.2$ ppm. EI MS (70 eV): m/z (%):

385 (M⁺, 12), 220 (100). Anal. calcd. for C₂₄H₁₆ClNO₂: C, 74.71; H, 4.18; N, 3.63. Found: C, 74.93; H, 4.02; N, 3.83.

(1E,4E)-1-(2-Butoxyquinolin-3-yl)-5-(4-methoxyphenyl)penta-1,4-dien-3-one 17i

Yellow solid, m.p. 123–125°C; FTIR (ATR) $\nu = 1668$ (C=O) cm^{-1} . ^1H NMR (400 MHz, CDCl₃) $\delta = 1.09$ (t, $J = 8.0$ Hz, 3H, CH₃), 1.60–1.70 (m, 2H, CH₂), 1.92–2.02 (m, 2H, CH₂), 3.89 (s, 3H, OCH₃), 4.63 (t, $J = 8.0$ Hz, 2H, OCH₂), 6.98 (d, $J = 8.0$ Hz, 2H), 7.00 (d, $J = 16.0$ Hz, 1H, =CH), 7.42 (t, $J = 8.0$ Hz, 1H), 7.46 (d, $J = 16.0$ Hz, 1H, =CH), 7.61 (d, $J = 8.0$ Hz, 2H), 7.67 (t, $J = 8.0$ Hz, 1H), 7.76 (d, $J = 16.0$ Hz, 1H, =CH), 7.77 (s, 1H), 7.85 (d, $J = 8.0$ Hz, 1H), 7.98 (d, $J = 16.0$ Hz, 1H, =CH), 8.26 (s, 1H) ppm. ^{13}C NMR (101 MHz, CDCl₃) $\delta = 14.0, 19.6, 31.1, 55.5, 66.6, 114.5, 120.4, 123.8, 124.6, 125.0, 127.0, 127.6, 128.0, 128.3, 130.2, 130.7, 137.4, 138.8, 143.3, 146.8, 160.1, 160.7, 189.2$ ppm. EI MS (70 eV): m/z (%): 387 (M⁺, 14), 314 (11), 302 (10), 170 (100), 133 (24), 41 (31). Anal. calcd. for C₂₅H₂₅NO₃: C, 77.49; H, 6.50; N, 3.61. Found: C, 77.30; H, 6.67; N, 3.42.

(1E,4E)-1-(2-Butoxy-6-methylquinolin-3-yl)-5-(4-chlorophenyl)penta-1,4-dien-3-one 17j

Yellow solid, m.p. 120–125°C; FTIR (ATR) $\nu = 1670$ (C=O) cm^{-1} . ^1H NMR (400 MHz, CDCl₃) $\delta = 1.08$ (t, $J = 8.0$ Hz, 3H, CH₃), 1.55–1.70 (m, 2H, CH₂), 1.90–2.00 (m, 2H, CH₂), 2.51 (s, 3H, CH₃), 4.60 (t, $J = 8.0$ Hz, 2H, OCH₂), 7.07 (d, $J = 16.0$ Hz, 1H, =CH), 7.42 (d, $J = 8.0$ Hz, 2H), 7.46 (d, $J = 16.8$ Hz, 1H, =CH), 7.47–7.54 (m, 2H), 7.56 (d, $J = 8.0$ Hz, 2H), 7.71 (d, $J = 16.0$ Hz, 1H, =CH), 7.75 (s, 1H), 7.97 (d, $J = 16.0$ Hz, 1H, =CH), 8.16 (s, 1H) ppm. ^{13}C NMR (101 MHz, CDCl₃) $\delta = 14.0, 19.6, 21.3, 31.2, 66.3, 119.9, 124.9, 126.2, 126.8, 127.1, 127.8, 129.3, 129.5, 132.9, 133.4, 134.2, 136.4, 138.5, 138.5, 141.8, 145.4, 159.6, 189.0$ ppm. EI MS (70 eV): m/z (%): 407/405 (M⁺, 2/6), 240 (20), 202 (19), 184 (100), 159 (50), 130 (23), 41 (19). Anal. calcd. for C₂₅H₂₄ClNO₂: C, 73.97; H, 5.96; N, 3.45. Found: C, 80.12; H, 6.08; N, 3.21.

(1E,4E)-1-(2-Butoxy-8-methylquinolin-3-yl)-5-(4-hydroxy-3-methoxyphenyl)penta-1,4-dien-3-one 17k

Yellow solid, m.p. 142–143°C. FTIR (ATR): $\nu = 3320$ (OH), 1662, (C=O) cm^{-1} . ^1H NMR (400 MHz, CDCl₃) $\delta = 1.09$ (t, $J = 7.4$ Hz, 3H, CH₃), 1.70–1.54 (m, 2H, CH₂), 2.02–1.85 (m, 2H, CH₂), 2.72 (s, 3H, CH₃), 3.99 (s, 3H, OCH₃), 4.65 (t, $J = 6.6$ Hz, 2H, OCH₂), 6.03 (s, 1H, OH), 6.97 (d, $J = 15.9$ Hz, 1H, =CH), 7.00 (d, $J = 8.2$ Hz, 1H), 7.16 (d, $J = 1.8$ Hz, 1H), 7.22 (dd, $J = 8.2, 1.8$ Hz, 1H), 7.30 (s, 1H), 7.32 (d, $J = 7.6$ Hz, 1H), 7.49 (d, $J = 16.0$ Hz, 1H, =CH), 7.53 (d, $J = 7.0$ Hz, 1H), 7.62 (d, $J = 8.0$ Hz, 1H), 7.73 (d, $J = 15.9$ Hz, 1H, =CH), 7.99 (d, $J = 16.0$ Hz, 1H, =CH), 8.23 (s, 1H). ^{13}C NMR (101 MHz, CDCl₃) $\delta = 9.3, 12.9, 14.9, 26.3, 51.3, 61.5, 105.0, 110.2, 115.0, 118.8, 119.2, 119.4, 120.01, 121.1, 122.7, 123.1, 126.1, 130.5, 133.0, 134.4, 139.9, 140.9, 142.2, 143.6, 154.3, 184.5$ ppm. EI MS (70 eV): m/z (%): 417 (M⁺, 17), 212 (62), 184 (100), 172 (51). Anal. calcd. for C₂₆H₂₇NO₄: C, 74.80; H, 6.52; N, 3.35. Found: C, 74.63; H, 6.35; N, 3.53.

(1E,4E)-1-(2-Butoxy-7-chloroquinolin-3-yl)-5-(4-hydroxy-3-methoxyphenyl)penta-1,4-dien-3-one 17l

Yellow solid, m.p. 130–131°C. FTIR (ATR): $\nu = 3315$ (OH), 1660 (C=O) cm^{-1} . ^1H NMR (400 MHz, CDCl_3) $\delta = 1.08$ (t, $J = 7.4$ Hz, 3H, CH_3), 1.68–1.56 (m, 2H, CH_2), 2.00–1.89 (m, 2H, CH_2), 3.98 (s, 3H, OCH_3), 4.60 (t, $J = 6.6$ Hz, 2H, OCH_2), 6.95 (d, $J = 15.9$ Hz, 1H, =CH), 6.99 (d, $J = 8.2$ Hz, 1H), 7.14 (d, $J = 1.7$ Hz, 1H), 7.20 (dd, $J = 8.2$, 1.8 Hz, 1H), 7.30 (s, 1H), 7.36 (dd, $J = 8.6$, 2.0 Hz, 1H), 7.45 (d, $J = 16.0$ Hz, 1H, =CH), 7.68 (d, $J = 8.7$ Hz, 1H), 7.72 (d, $J = 16.0$ Hz, 1H, =CH), 7.84 (d, $J = 1.9$ Hz, 1H), 7.93 (d, $J = 16.0$ Hz, 1H, =CH), 8.20 (s, 1H). ^{13}C NMR (101 MHz, CDCl_3) $\delta = 14.0$, 19.6, 31.1, 56.0, 66.7, 109.8, 115.0, 120.5, 123.3, 123.6, 123.8, 125.4, 126.3, 127.3, 128.2, 129.0, 136.6, 137.1, 138.2, 143.9, 146.9, 147.4, 148.4, 160.7, 189.1 ppm. EI MS (70 eV): m/z (%): 437 (M^+ , 3), 204 (14), 129 (16), 57 (99), 43 (100). Anal. calcd. for $\text{C}_{25}\text{H}_{24}\text{ClNO}_4$: C, 68.57; H, 5.52; N, 3.20. Found: C, 68.80; H, 5.25; N, 3.09.

1-Butyl-6-chloro-3-((1E,4E)-5-(4-methoxyphenyl)-3-oxopenta-1,4-dien-1-yl)quinolin-2(1H)-one 17m

Yellow solid, m.p. 177–179°C. FTIR (ATR) $\nu = 1649$, 1601 (C=O) cm^{-1} . ^1H NMR (CDCl_3) $\delta = 1.06$ (t, $J = 8.0$ Hz, 3H, CH_3), 1.50–1.62 (m, 2H, CH_2), 1.75–1.83 (m, 2H, CH_2), 3.89 (s, 3H, OCH_3) 4.36 (t, $J = 8.0$ Hz, 2H, NCH_2), 6.96 (d, $J = 8.0$ Hz, 2H), 7.02 (d, $J = 16.0$ Hz, 1H, =CH), 7.34 (d, $J = 12.0$ Hz, 1H), 7.55–7.66 (m, 3H), 7.66 (d, $J = 4.0$ Hz, 1H), 7.77 (d, $J = 16.0$ Hz, 1H, =CH), 7.77 (d, $J = 16.0$ Hz, 1H, =CH), 7.90 (d, $J = 16.0$ Hz, 1H, =CH), 7.90 (s, 1H) ppm; ^{13}C NMR (101 MHz, CDCl_3) $\delta = 13.9$, 20.4, 29.6, 43.0, 56.1, 114.5, 115.7, 121.5, 123.9, 127.5, 127.6, 127.8, 128.6, 129.7, 130.2, 131.6, 137.5, 137.6, 139.2, 143.5, 160.4, 161.7, 189.6 ppm. EI MS (70 eV): m/z (%): 423/421 (M^+ , 8/21), 260 (76), 204 (66), 161 (45), 133 (59), 84 (100), 48 (17). Anal. calcd. for $\text{C}_{25}\text{H}_{24}\text{ClNO}_3$: C, 71.17; H, 8.40; N, 3.32. Found: C, 71.30; H, 8.51; N, 3.21.

1-Butyl-7-chloro-3-((1E,4E)-5-(4-hydroxy-3-methoxyphenyl)-3-oxopenta-1,4-dien-1-yl)quinolin-2(1H)-one 17n

Yellow solid, m.p. 194–195°C. FTIR (ATR): $\nu = 3322$ (OH), [1651, 1643] (C=O) cm^{-1} . ^1H NMR (400 MHz, CDCl_3) $\delta = 1.07$ (t, $J = 7.3$ Hz, 3H, CH_3), 1.63–1.47 (m, 2H, CH_2), 1.85–1.70 (m, 2H, CH_2), 3.98 (s, 3H, OCH_3), 4.35–4.25 (m, 2H, NCH_2), 6.98 (s, 1H), 6.98 (d, $J = 15.84$ Hz, 1H, =CH), 7.16 (d, $J = 6.5$ Hz, 1H), 7.18 (d, $J = 8.3$ Hz, 1H), 7.25 (d, $J = 8.0$ Hz, 1H), 7.37 (d, $J = 1.1$ Hz, 1H), 7.59 (d, $J = 8.3$ Hz, 1H), 7.72 (d, $J = 15.8$ Hz, 1H, =CH), 7.74 (d, $J = 15.7$ Hz, 1H, =CH), 7.91 (d, $J = 15.8$ Hz, 1H, =CH), 7.93 (s, 1H). ^{13}C NMR (101 MHz, CDCl_3) $\delta = 13.9$, 20.4, 29.5, 43.0, 56.1, 109.6, 114.3, 114.9, 119.0, 123.0, 123.9 ($\times 2$), 126.2, 127.4, 129.2, 130.8, 137.7, 138.6, 139.8, 140.2, 143.9, 146.9, 148.4, 160.6, 189.6 ppm. EI MS (70 eV): m/z (%): 437 (M^+ , 5), 341 (44), 313 (29), 260 (100), 204 (67). Anal. calcd. for $\text{C}_{25}\text{H}_{24}\text{ClNO}_4$: C, 68.57; H, 5.52; N, 3.20. Found: C, 68.81; H, 5.31; N, 3.03.

1-Benzyl-7-chloro-3-((1E,4E)-5-(4-hydroxy-3-methoxyphenyl)-3-oxopenta-1,4-dien-1-yl)quinolin-2(1H)-one 17o

Yellow solid, m.p. 190–191°C. FTIR (ATR): $\nu = 3312$ (OH), [1660, 1645] (C=O) cm^{-1} . ^1H NMR (400 MHz, CDCl_3) $\delta = 3.98$ (s, 3H,

OCH_3), 5.60 (s, 2H, Ph-CH_2), 6.97 (d, $J = 7.9$ Hz, 1H), 6.99 (d, $J = 15.8$ Hz, 1H, =CH), 7.16 (s, 1H), 7.19 (d, $J = 8.1$ Hz, 1H), 7.23 (d, $J = 5.9$ Hz, 1H), 7.45–7.25 (m, 7H), 7.61 (d, $J = 5.7$ Hz, 1H), 7.74 (d, $J = 15.5$ Hz, 1H, =CH), 7.80 (d, $J = 15.4$ Hz, 1H, =CH), 7.98 (d, $J = 15.8$ Hz, 1H, =CH), 8.02 (s, 1H). ^{13}C NMR (101 MHz, CDCl_3) $\delta = 46.6$, 56.1, 109.7, 114.9, 115.0, 119.0, 123.4, 123.9, 124.0, 126.3, 126.5, 127.4, 127.7, 129.1, 129.4, 130.8, 135.4, 137.6, 138.2, 140.1, 140.7, 144.0, 146.9, 148.4, 161.0, 189.6 ppm. EI MS (70 eV): m/z (%): 471 (M^+ , 3), 294 (10), 91 (100). Anal. calcd. for $\text{C}_{28}\text{H}_{22}\text{ClNO}_4$: C, 71.26; H, 4.70; N, 2.97. Found: C, 71.51; H, 5.01; N, 3.15.

(1E,4E)-1-(2-(Benzyloxy)-7-chloroquinolin-3-yl)-5-(4-hydroxy-3-methoxyphenyl)penta-1,4-dien-3-one 17p

Yellow solid, m.p. 152–153°C. FTIR (ATR): $\nu = 3320$ (OH), 1670 (C=O) cm^{-1} . ^1H NMR (400 MHz, CDCl_3) $\delta = 3.97$ (s, 3H, OCH_3), 5.68 (s, 2H, Ph-CH_2), 6.01 (s, 1H, OH), 6.87 (d, $J = 15.9$ Hz, 1H, =CH), 6.98 (d, $J = 8.0$ Hz, 1H), 7.08 (s, 1H), 7.10 (d, $J = 8.6$ Hz, 1H), 7.37 (t, $J = 4.9$ Hz, 1H), 7.40 (d, $J = 7.5$ Hz, 2H), 7.45 (t, $J = 7.5$ Hz, 2H), 7.50 (d, $J = 16.2$ Hz, 1H, =CH), 7.58 (d, $J = 16.3$ Hz, 1H, =CH), 7.62 (d, $J = 7.4$ Hz, 2H), 7.71 (d, $J = 8.6$ Hz, 1H), 7.89 (d, $J = 1.6$ Hz, 1H, =CH), 7.94 (d, $J = 15.9$ Hz, 1H, =CH), 8.23 (s, 1H). ^{13}C NMR (101 MHz, CDCl_3) $\delta = 56.0$, 68.6, 109.6, 114.9, 120.5, 123.6, 123.8, 124.0, 125.7, 126.4, 127.3, 128.1, 128.3, 128.3, 128.6, 129.1, 136.7, 136.8, 136.9, 138.8, 143.9, 146.9, 147.1, 148.4, 160.3, 189.0 ppm. EI MS (70 eV): m/z (%): 473/471 (M^+ , 5/14), 380 (15), 236 (25), 149 (56), 92 (100). Anal. calcd. for $\text{C}_{28}\text{H}_{22}\text{ClNO}_4$: C, 71.26; H, 4.70; N, 2.97. Found: C, 71.46; H, 4.48; N, 2.72.

(1E,4E)-1-(2-(Benzyloxy)benzo[h]quinolin-3-yl)-5-(4-chlorophenyl)-penta-1,4-dien-3-one 17q

Yellow solid, m.p. 150–153°C. FTIR (ATR): $\nu = 1672$ (C=O) cm^{-1} . ^1H NMR (400 MHz, $\text{DMSO}-d_6$) $\delta = 5.78$ (s, 2H, Ph-CH_2), 7.23 (d, $J = 16.0$ Hz, 1H, =CH), 7.30–8.05 (m, 17H, Ar-H , =CH), 8.76 (s, 1H), 9.05 (brs, 1H) ppm; ^{13}C NMR (101 MHz, $\text{DMSO}-d_6$) $\delta = 68.3$, 119.1, 122.5, 124.8, 125.7, 126.0, 127.3, 127.5, 128.0, 128.0, 128.4, 128.6, 129.0, 129.1, 129.5, 130.1, 130.6, 134.0, 134.5, 135.6, 136.7, 137.7, 139.2, 142.0, 144.6, 159.3, 188.8 ppm. EI MS (70 eV): m/z (%): 477/475 (M^+ , 3/8), 368 (10), 310 (63), 165 (22), 91 (100). Anal. calcd. for $\text{C}_{31}\text{H}_{22}\text{ClNO}_2$: C, 78.23; H, 4.66; N, 2.94. Found: C, 78.04; H, 4.83; N, 3.10.

(1E,4E)-1-(2-(Benzyloxy)benzo[h]quinolin-3-yl)-5-(4-methoxyphenyl)-penta-1,4-dien-3-one 17r

Yellow solid, m.p. 155–157°C; FTIR (ATR): $\nu = 1647$ (C=O) cm^{-1} . ^1H NMR (400 MHz, $\text{DMSO}-d_6$) $\delta = 3.83$ (s, 3H, OCH_3), 5.80 (s, 2H, Ph-CH_2), 7.04 (d, $J = 8.0$ Hz, 2H), 7.09 (d, $J = 16.0$ Hz, 1H, =CH), 7.36 (d, $J = 8.0$ Hz, 1H), 7.41 (d, $J = 16.0$ Hz, 1H, =CH), 7.46 (d, $J = 4.0$ Hz, 1H), 7.63–7.78 (m, 8H), 7.84 (d, $J = 4.0$ Hz, 2H), 7.96 (d, $J = 16.0$ Hz, 1H, =CH), 7.99–8.03 (m, 1H), 8.81 (s, 1H), 9.05–9.10 (m, 1H) ppm; ^{13}C NMR (101 MHz, $\text{DMSO}-d_6$) $\delta = 55.9$, 68.3, 115.0, 119.3, 122.5, 124.7, 124.8, 125.7, 125.9, 127.3, 127.6, 128.1, 128.4, 128.6, 129.0, 129.1, 130.1, 130.9, 134.5, 136.4, 137.7,

138.9, 143.5, 144.5, 159.4, 161.9, 188.6 ppm; EI MS (70 eV): *m/z* (%): 471 (M^+ , 26), 364 (36), 310 (63), 219 (17), 161 (98), 133 (42), 91 (100). Anal. calcd. for $C_{33}H_{36}N_2O_3$: C, 77.92; H, 7.13; N, 5.51. Found: C, 78.12; H, 7.34; N, 5.22.

3-((1*E*,4*E*)-5-(Benzo[d][1,3]dioxol-5-yl)-3-oxopenta-1,4-dien-1-yl)-1-butyl-7-chloroquinolin-2(1*H*)-one 17s

Yellow solid, m.p. 200–202°C; FTIR (ATR): ν = [1653, 1597] (C=O) cm^{-1} . 1H NMR (400 MHz, $CDCl_3$) δ = 1.07 (t, J = 8.0 Hz, 3H, CH_3), 1.50–1.62 (m, 2H, CH_2), 1.70–1.83 (m, 2H, CH_2), 4.32 (t, J = 8.0 Hz, 2H, NCH_2), 6.05 (s, 2H, CH_2), 6.86 (d, J = 8.0 Hz, 1H), 6.95 (d, J = 16.0 Hz, 1H, =CH), 7.10–7.15 (m, 2H), 7.25 (dd, J = 8.0 Hz, J = 4.0 Hz, 1H), 7.36 (d, J = 4.0 Hz, 1H), 7.58 (d, J = 8.0 Hz, 1H), 7.69 (d, J = 16.0 Hz, 1H, =CH), 7.74 (d, J = 16.0 Hz, 1H, =CH), 7.85 (d, J = 16.0 Hz, 1H, =CH), 7.93 (s, 1H) ppm; ^{13}C NMR (101 MHz, $CDCl_3$) δ = 13.9, 20.4, 29.5, 43.0, 101.6, 106.7, 108.7, 114.3, 119.0, 123.0, 124.1, 125.1, 126.2, 129.2, 129.3, 130.8, 137.8, 138.0, 139.9, 139.9, 143.3, 148.4, 149.9, 180.6, 189.5 ppm. MS (70 eV) *m/z* (%): 437/435 (3.7/7.8, M^+), 260 (100), 206/204 (43/95), 94 (95), 57 (75), 41 (33). Anal. calcd. for $C_{25}H_{22}ClNO_4$: C, 68.89; H, 5.09; N, 3.21. Found: C, 69.03; H, 4.86; N, 3.46.

(1*E*,4*E*)-1-(Benzo[d][1,3]dioxol-5-yl)-5-(2-butoxy-6-chloroquinolin-3-yl)penta-1,4-dien-3-one 17t

Yellow solid, m.p. 191–193°C; FTIR (ATR): ν = 1649 (C=O) cm^{-1} . 1H NMR (400 MHz, $CDCl_3$) δ = 1.08 (t, J = 8.0 Hz, 3H, CH_3), 1.56–1.72 (m, 2H, CH_2), 1.90–2.00 (m, 2H, CH_2), 4.62 (t, J = 8.0 Hz, 2H, NCH_2), 6.07 (s, 2H), 6.89 (d, J = 8.0 Hz, 1H), 6.95 (d, J = 16.0 Hz, 1H, =CH), 7.14 (d, J = 8.0 Hz, 1H), 7.17 (s, 1H), 7.43 (d, J = 16.0 Hz, 1H, =CH), 7.60 (dd, J = 2.0 Hz, J = 8.8 Hz, 1H), 7.71 (d, J = 16.0 Hz, 1H, =CH), 7.76 (d, J = 4.0 Hz, 1H), 7.78 (d, J = 8.0 Hz, 1H), 7.95 (d, J = 16.0 Hz, 1H, =CH), 8.17 (s, 1H) ppm. ^{13}C NMR (101 MHz, $CDCl_3$) δ = 14.0, 19.6, 31.1, 66.7, 101.7, 106.6, 108.7, 121.3, 123.9, 125.2, 125.6, 126.6, 128.6, 128.9, 129.3, 129.9, 131.2, 137.0, 137.4, 143.5, 145.3, 148.5, 150.0, 160.2, 188.9 ppm. EI MS (70 eV) *m/z* (%): 437/435 (11/31, M^+), 381/379 (8/26), 206/204 (36/100), 175 (29), 145 (37), 89 (32). Anal. calcd. for $C_{25}H_{22}ClNO_4$: C, 68.89; H, 5.09; N, 3.21. Found: C, 68.68; H, 5.23; N, 2.98.

(1*E*,4*E*)-1-(2-Butoxy-6-chloroquinolin-3-yl)-5-(4-chlorophenyl)penta-1,4-dien-3-one 17u

Yellow solid, m.p. 160–164°C. FTIR (ATR) ν = 1655 (C=O) cm^{-1} . 1H NMR (400 MHz, $CDCl_3$) δ = 1.08 (t, J = 8.0 Hz, 3H, CH_3), 1.57–1.68 (m, 2H, CH_2), 1.90–2.00 (m, 2H, CH_2), 4.61 (t, J = 8.0 Hz, 2H, OCH_2), 7.07 (d, J = 16.0 Hz, 1H, =CH), 7.43 (d, J = 4.0 Hz, J = 12.0 Hz, 3H), 7.59 (d, J = 16.0 Hz, 1H, =CH), 7.60 (d, J = 9.6 Hz, 2H), 7.73 (d, J = 16.0 Hz, 1H, =CH), 7.78 (d, J = 8.0 Hz, 2H), 7.95 (d, J = 16.0 Hz, 1H, =CH), 8.16 (s, 1H) ppm; ^{13}C NMR (101 MHz, $CDCl_3$) δ = 14.0, 19.6, 31.1, 66.7, 121.1, 125.5, 126.1, 126.6, 128.6, 128.6, 129.0, 129.3, 129.3, 129.5, 129.9, 131.3, 133.3, 136.6, 137.6, 142.1, 145.4, 160.2, 188.8 ppm. EI MS (70 eV) *m/z* (%): 425 (M^+ , 18), 260 (42), 204 (100), 165 (64), 137 (68), 102 (66), 69 (97), 41 (81). Anal. calcd. for

$C_{24}H_{21}Cl_2NO_2$: C, 67.61; H, 4.97; N, 3.29. Found: C, 67.78; H, 5.10; N, 3.05.

(1*E*,4*E*)-1-(2-Butoxy-6-chloroquinolin-3-yl)-5-(4-methoxyphenyl)penta-1,4-dien-3-one 17v

Yellow solid. Mp. 125–128°C; FTIR (ATR) ν = 1649 (C=O) cm^{-1} . 1H NMR ($CDCl_3$) δ = 1.08 (t, J = 8.0 Hz, 3H, CH_3), 1.58–1.67 (m, 2H, CH_2), 1.90–1.98 (m, 2H, CH_2), 3.88 (s, 3H, OCH_3), 4.59 (t, J = 8.0 Hz, 2H, OCH_2), 6.96 (d, J = 8.0 Hz, 2H), 6.97 (d, J = 16.0 Hz, 1H, =CH), 7.43 (d, J = 16.0 Hz, 1H, =CH), 7.54–7.62 (m, 3H), 7.70–7.78 (m, 3H), 7.92 (d, J = 16.0 Hz, 1H, =CH), 8.12 (s, 1H, Quin-H) ppm; ^{13}C NMR ($CDCl_3$) δ = 14.0, 19.6, 31.1, 55.4, 66.6, 114.5, 121.3, 123.7, 125.6, 126.5, 127.5, 128.5, 128.8, 129.8, 130.2, 131.1, 136.8, 137.4, 143.5, 145.2, 160.2, 161.8, 189.0 ppm. EI MS (70 eV) *m/z* (%): 423/421 (20/52, M^+), 348 (42), 204 (100), 161 (77), 133 (51), 94 (77), 57 (55), 41 (49). Anal. calcd. for $C_{25}H_{24}ClNO_3$: C, 71.17; H, 5.73; N, 3.32. Found: C, 71.02; H, 6.81; N, 3.10.

(1*E*,4*E*)-1-(Benzo[d][1,3]dioxol-5-yl)-5-(2-butoxy-6-methylquinolin-3-yl)penta-1,4-dien-3-one 17w

Yellow solid, m.p. 160–162°C. FTIR (ATR) ν = 1647 (C=O) cm^{-1} . 1H NMR (101 MHz, $CDCl_3$) δ = 1.08 (t, J = 8.0 Hz, 3H, CH_3), 1.57–1.70 (m, 2H, CH_2), 1.90–2.00 (m, 2H, CH_2), 2.53 (s, 3H, CH_3), 4.62 (t, J = 8.0 Hz, 2H, CH_2), 6.07 (s, 2H), 6.88 (d, J = 8.0 Hz, 1H), 6.95 (d, J = 16.0 Hz, 1H, =CH), 7.14 (dd, J = 8.0 Hz, J = 1.2 Hz, 1H), 7.17 (d, J = 1.2 Hz, 1H), 7.43 (d, J = 16.0 Hz, 1H, =CH), 7.51 (dd, J = 1.6 Hz, J = 8.0 Hz, 1H), 7.54 (s, 1H), 7.71 (d, J = 16.0 Hz, 1H, =CH), 7.77 (d, J = 12.0 Hz, 1H), 7.97 (d, J = 16.0 Hz, 1H, =CH), 8.18 (s, 1H) ppm. ^{13}C NMR (101 MHz, $CDCl_3$) δ = 14.0, 19.7, 21.3, 31.2, 66.5, 101.7, 106.6, 108.7, 120.1, 124.0, 124.9, 125.1, 126.7, 127.1, 128.1, 129.4, 132.9, 134.2, 137.8, 138.4, 143.2, 145.2, 148.5, 149.9, 159.7, 189.1 ppm. EI MS (70 eV) *m/z* (%): 415 (28), 184 (100), 172 (42), 89 (38). Anal. calcd. for $C_{26}H_{25}NO_4$: C, 75.16; H, 6.07; N, 3.37. Found: C, 75.28; H, 5.88; N, 3.51.

4.2 | Anticancer activity

The human cancer cell lines of the cancer screening panel were grown in an RPMI-1640 medium containing 5% fetal bovine serum and 2 mM L-glutamine. For a typical screening experiment, cells were inoculated into 96-well microtiter plates. After cell inoculation, the microtiter plates were incubated at 37°C, 5% CO_2 , 95% air, and 100% relative humidity for 24 h before the addition of the tested compounds. After 24 h, two plates of each cell line were fixed in situ with trichloroacetic acid (TCA), to represent a measurement of the cell population for each cell line at the time of sample addition (Tz). The samples were solubilized in DMSO at 400-fold the desired final maximum test concentration and stored frozen before use. At the time of compound addition, an aliquot of frozen concentrate was thawed and diluted to twice the desired final maximum test concentration with a complete medium containing 50 $\mu g/ml$ gentamicin. An additional four 10-fold or

1/2 log serial dilutions were made to provide a total of five drug concentrations plus the control. Aliquots of 100 μ l of these different sample dilutions were added to the appropriate microtiter wells already containing 100 μ l of medium, resulting in the required final sample concentrations.^[32] After the tested compounds were added, the plates were incubated for an additional 48 h at 37°C, 5% CO₂, 95% air, and 100% relative humidity. For adherent cells, the assay was terminated by the addition of cold TCA. Cells were fixed in situ by the gentle addition of 50 μ l of cold 50% (w/v) TCA (final concentration, 10% TCA) and incubated for 60 min at 4°C. The supernatant was discarded, and plates were washed five times with tap water and air-dried. SRB solution (100 μ l) at 0.4% (w/v) in 1% acetic acid was added to each well, and plates were incubated for 10 min at room temperature. After staining, the unbound dye was removed by washing five times with 1% acetic acid and the plates were air-dried. The bound stain was subsequently solubilized with 10 mM Trizma base, and the absorbance was read on an automated plate reader at a wavelength of 515 nm. Using the seven absorbance measurements (time zero [Tz], control growth in the absence of drug [C], and test growth in the presence of drug at the five concentration levels [Ti]), the percentage growth was calculated at each of the drug concentrations levels. Percentage growth inhibition was calculated as follows: $[(Ti - Tz)/(C - Tz)] \times 100$ for concentrations for which $Ti > Tz$, and $[(Ti - Tz)/Tz] \times 100$ for concentrations for which $Ti < Tz$. Two dose-response parameters were calculated for each compound. Growth inhibition of 50% (GI₅₀) was calculated from $[(Ti - Tz)/(C - Tz)] \times 100 = 50$, which is the drug concentration resulting in a 50% lower net protein increase in the treated cells (measured by SRB staining) as compared with the net protein increase seen in the control cells and the LC₅₀ (concentration of drug resulting in a 50% reduction in the measured protein at the end of the drug treatment as compared with that at the beginning), indicating a net loss of cells, calculated from $[(Ti - Tz)/Tz] \times 100 = -50$. Values were calculated for each of these two parameters if the level of activity was reached; however, if the effect was not reached or was exceeded, the value for that parameter was expressed as greater or less than the maximum or minimum concentration tested.^[32,33]

4.3 | Computational methods

B3LYP/6-31G*^[36,37] geometry optimizations were performed with the Gaussian 09 package of programs.^[38] Molecular docking calculations for modeling the binding modes and evaluating the interaction energies of selected compounds as ligands for several enzymes were carried out with AutoDock Vina (version 1.1.2),^[39] using default parameters. The three-dimensional coordinates of the proteins were obtained from the RCSB Protein Data Bank (PDB IDs: 3PP0^[40] (HER2), 3SDK^[41] (20S proteasome), 4AG8^[42] (VEGFR2), 4XV2^[43] (BRAF), 4LVT^[44] (Bcl-2), 5XDL^[45] (HER1), and 5X5D^[46] (hTS)). Chain A of HER2, VEGFR2, BRAF, Bcl-2, HER1, and hTS, and chains K (β 5 subunit) and L (β 6 subunit) of 20S proteasome were selected as target templates for the docking

computations. Co-crystallized ligands and crystallographic water molecules were removed. The addition of hydrogens, merger of nonpolar hydrogens to the atom to which they were linked, and the assignment of partial charges were computed with AutoDockTools. Docking areas were constrained to a 30 \times 30 \times 30 Å box centered at the active site of the proteins, providing proper space for rotational and translational movement of the ligands. The most stable docking pose for each compound was selected to determine its binding affinity.

ACKNOWLEDGMENTS

The authors thank COLCIENCIAS, Universidad del Valle—Project Number 110680864255, and Universidad del Norte for financial support, and “Centro de Instrumentación Científico-Técnica of Universidad de Jaén” for data collection. This study also was supported in part by the Spanish Ministerio de Ciencia, Innovación y Universidades, project #RTI2018-098560-B-C22, Universidad de Jaén, Consejería de Innovación, Ciencia y Empresa (Junta de Andalucía, Spain).

ORCID

Rodrigo Abonia  <http://orcid.org/0000-0003-3256-0961>

Braulio Insuasty  <http://orcid.org/0000-0001-8371-3310>

REFERENCES

- [1] P. Singh, A. Anand, V. Kumar, *Eur. J. Med. Chem.* **2014**, *85*, 758.
- [2] R. Abonia, D. Insuasty, J. Castillo, B. Insuasty, J. Quiroga, M. Nogueiras, J. Cobo, *Eur. J. Med. Chem.* **2012**, *57*, 29.
- [3] B. Mathew, J. Suresh, S. Anbazhagan, J. Paulraj, G. K. Krishnan, *Biomed. Prev. Nutr.* **2014**, *4*, 451.
- [4] J. Menezes, M. F. Diederich, *Eur. J. Med. Chem.* **2019**, *182*, 111637.
- [5] D. Insuasty, S. Robledo, I. D. Vélez, P. Cuervo, B. Insuasty, J. Quiroga, M. Nogueiras, J. Cobo, R. Abonia, *Eur. J. Med. Chem.* **2017**, *141*, 567.
- [6] W. Dan, J. Dai, *Eur. J. Med. Chem.* **2020**, *187*, 111980.
- [7] L. De Carvalho Tavares, S. Johann, T. M. De Almeida Alves, J. C. Guerra, E. M. De Souza-Fagundes, P. S. Cisalpino, A. J. Bortoluzzi, G. F. Caramori, R. De Mattos Piccoli, H. T. S. Braibante, M. E. F. Braibante, M. G. Pizzolatti, *Eur. J. Med. Chem.* **2011**, *46*, 4448.
- [8] D. Ramesh, A. Joji, B. G. Vijayakumar, A. Sethumadhavan, M. Mani, T. Kannan, *Eur. J. Med. Chem.* **2020**, *198*, 112358.
- [9] R. H. Hans, E. M. Guantai, C. Lategan, P. J. Smith, B. Wan, S. G. Franzblau, J. Gut, P. J. Rosenthal, K. Chibale, *Bioorg. Med. Chem. Lett.* **2010**, *20*, 942.
- [10] A. Özdemir, M. D. Altintop, G. Turan-Zitouni, G. A. Çiftçi, Ö. Ertoran, Ö. Alataş, Z. A. Kaplancikli, *Eur. J. Med. Chem.* **2015**, *89*, 304.
- [11] M. Liu, P. Wilairat, S. L. Croft, A. L. C. Tan, M. L. Go, *Bioorg. Med. Chem.* **2003**, *11*, 2729.
- [12] H. Mirzaei, S. Emami, *Eur. J. Med. Chem.* **2016**, *121*, 610.
- [13] S. A. Nouredin, R. M. El-Shishtawy, K. O. Al-Footy, *Eur. J. Med. Chem.* **2019**, *182*, 111631.
- [14] Z. Rafiee, M. Nejatian, M. Daeihamed, S. M. Jafari, *Trends Food Sci. Technol.* **2019**, *88*, 445.
- [15] S. Abrahams, W. L. Haylett, G. Johnson, J. A. Carr, S. Bardien, *Neuroscience* **2019**, *406*, 1.
- [16] C. Selvam, S. L. Prabu, B. C. Jordan, Y. Purushothaman, A. Umamaheswari, M. S. Hosseini Zare, R. Thilagavathi, *Life Sci.* **2019**, *239*, 117032.
- [17] S. Zhao, C. Pi, Y. Ye, L. Zhao, Y. Wei, *Eur. J. Med. Chem.* **2019**, *180*, 524.

- [18] M. J. Banez, M. I. Geluz, A. Chandra, T. Hamdan, O. S. Biswas, N. S. Bryan, E. R. Von Schwarz, *Nutr. Res.* **2020**, *78*, 11.
- [19] G. L. Borosky, K. K. Laali, *Mini-Rev. Med. Chem.* **2020**, *20*, 1543.
- [20] C. Y. Hsieh, P. W. Ko, Y. J. Chang, M. Kapoor, Y. C. Liang, H. L. Chu, H. H. Lin, J. C. Horng, M. H. Hsu, *Molecules* **2019**, *24*, 3259.
- [21] M. Hossain, S. Das, U. Das, A. Doroudi, J. Zhu, J. R. Dimmock, *Bioorg. Med. Chem. Lett.* **2020**, *30*, 126878.
- [22] S. Jain, V. Chandra, P. Kumar Jain, K. Pathak, D. Pathak, A. Vaidya, *Arab. J. Chem.* **2019**, *12*, 4920.
- [23] O. Afzal, S. Kumar, M. R. Haider, M. R. Ali, R. Kumar, M. Jaggi, S. Bawa, *Eur. J. Med. Chem.* **2015**, *97*, 871.
- [24] L. M. Nainwal, S. Tasneem, W. Akhtar, G. Verma, M. F. Khan, S. Parvez, M. Shaquiquzzaman, M. Akhter, M. M. Alam, *Eur. J. Med. Chem.* **2019**, *164*, 121.
- [25] F. Gao, X. Zhang, T. Wang, J. Xiao, *Eur. J. Med. Chem.* **2019**, *165*, 59.
- [26] S. Raghavan, P. Manogaran, K. K. Gadepalli Narasimha, B. Kalpattu Kuppasami, P. Mariyappan, A. Gopalakrishnan, G. Venkatraman, *Bioorg. Med. Chem. Lett.* **2015**, *25*, 3601.
- [27] C. W. Murray, D. C. Rees, *Nat. Chem.* **2009**, *1*, 187.
- [28] M. Vettorazzi, D. Insuasty, S. Lima, L. Gutiérrez, M. Noguerras, A. Marchal, R. Abonia, S. Andújar, S. Spiegel, J. Cobo, D. Enriz, *Bioorg. Chem.* **2020**, *94*, 103414.
- [29] J. Ramírez-Prada, S. M. Robledo, I. D. Vélez, M. Crespo, J. Quiroga, R. Abonia, A. Montoya, L. Svetaz, S. Zacchino, B. Insuasty, *Eur. J. Med. Chem.* **2017**, *131*, 237.
- [30] D. Insuasty, R. Abonia, B. Insuasty, J. Quiroga, K. Laali, M. Noguerras, J. Cobo, *ACS Comb. Sci.* **2017**, *19*, 555.
- [31] O. Meth-Cohn, B. Narine, *Tetrahedron Lett.* **1978**, *19*, 2045.
- [32] NCI-60 Screening Methodology, https://dtp.cancer.gov/discovery_development/nci-60/methodology.htm
- [33] M. R. Boyd, K. D. Padl, *Drug Dev. Res.* **1995**, *34*, 91.
- [34] S. V. Malhotra, V. Kumar, C. Velez, B. Zayas, *MedChemComm* **2014**, *5*, 1404.
- [35] K. K. Laali, W. J. Greves, A. T. Zwarycz, J. C. Smits, F. J. Troendle, G. L. Borosky, S. Akhtar, A. Manna, A. Paulus, A. Chanan-Khan, M. Nukaya, G. D. Kennedy, *ChemMedChem* **2018**, *13*, 1895.
- [36] A. D. Becke, *J. Chem Phys.* **2001**, *98*, 5649.
- [37] C. Lee, C. Hill, *Phys. Rev.* **1988**, *37*, 785.
- [38] Gaussian 09, Revision E.01, M. J. Frisch, G. W. Trucks, H. B. Schlegel, G. E. Scuseria, M. A. Robb, J. R. Cheeseman, G. Scalmani, V. Barone, B. Mennucci, G. A. Petersson, H. Nakatsuji, M. Caricato, X. Li, H. P. Hratchian, A. F. Izmaylov, J. Bloino, G. Zheng, J. L. Sonnenberg, M. Hada, M. Ehara, K. Toyota, R. Fukuda, J. Hasegawa, M. Ishida, T. Nakajima, Y. Honda, O. Kitao, H. Nakai, T. Vreven, J. A. Montgomery, Jr., J. E. Peralta, F. Ogliaro, M. Bearpark, J. J. Heyd, E. Brothers, K. N. Kudin, V. N. Staroverov, R. Kobayashi, J. Normand, K. Raghavachari, A. Rendell, J. C. Burant, S. S. Iyengar, J. Tomasi, M. Cossi, N. Rega, J. M. Millam, M. Klene, J. E. Knox, J. B. Cross, V. Bakken, C. Adamo, J. Jaramillo, R. Gomperts, R. E. Stratmann, O. Yazyev, A. J. Austin, R. Cammi, C. Pomelli, J. W. Ochterski, R. L. Martin, K. Morokuma, V. G. Zakrzewski, G. A. Voth, P. Salvador, J. J. Dannenberg, S. Dapprich, A. D. Daniels, Ö. Farkas, J. B. Foresman, J. V. Ortiz, J. Cioslowski, D. J. Fox, Gaussian, Inc., Wallingford, CT **2009**.
- [39] O. Trott, A. J. Olson, *J. Comput. Chem.* **2010**, *31*, 455.
- [40] K. Aertgeerts, R. Skene, J. Yano, B. Sang, H. Zou, G. Snell, A. Jennings, K. Iwamoto, N. Habuka, A. Hirokawa, T. Ishikawa, T. Tanaka, H. Miki, *J. Biol. Chem.* **2011**, *286*, 18756.
- [41] C. Blackburn, C. Barrett, J. L. Blank, F. J. Bruzzese, N. Bump, L. R. Dick, P. Fleming, K. Garcia, P. Hales, Z. Hu, M. Jones, J. X. Liu, D. S. Sappal, M. D. Sintchak, C. Tsu, K. M. Gigstad, *Bioorg. Med. Chem. Lett.* **2010**, *20*, 6581.
- [42] M. Mctigue, B. William, J. H. Chen, Y. Deng, J. Solowiej, R. S. Kania, *Natl. Acad. Sci. U. S. A.* **2012**, *109*, 18281.
- [43] C. Zhang, W. Spevak, Y. Zhang, E. A. Burton, Y. Ma, G. Habets, J. Zhang, J. Lin, T. Ewing, B. Matusow, G. Tsang, A. Marimuthu, H. Cho, G. Wu, W. Wang, D. Fong, H. Nguyen, S. Shi, P. Womack, M. Nespi, R. Shellooe, H. Carias, B. Powell, E. Light, L. Sanftner, J. Walters, J. Tsai, B. L. West, G. Visor, H. Rezaei, P. S. Lin, K. Nolop, P. N. Ibrahim, P. Hirth, G. Bollag, *Nature* **2015**, *526*, 583.
- [44] A. J. Souers, J. D. Levenson, E. R. Boghaert, S. L. Ackler, N. D. Catron, J. Chen, B. D. Dayton, H. Ding, S. H. Enschede, W. J. Fairbrother, D. C. S. Huang, S. G. Hymowitz, S. Jin, S. L. Khaw, P. J. Kovar, L. T. Lam, J. Lee, H. L. Maecker, K. C. Marsh, K. D. Mason, M. J. Mitten, P. M. Nimmer, A. Oleksijew, C. H. Park, C. M. Park, D. C. Phillips, A. W. Roberts, D. Sampath, J. F. Seymour, M. L. Smith, G. M. Sullivan, S. K. Tahir, C. Tse, M. D. Wendt, Y. Xiao, J. C., Xue, H., Zhang, R. A., Humerickhouse, S. H., Rosenberg, S. W., Elmore, *Nat. Med.* **2013**, *19*, 202.
- [45] X. Yan, S. Zhu, L. Liang, P. Zhao, H. G. Choi, *Oncotarget* **2017**, *8*, 53508.
- [46] D. Chen, A. Jansson, D. Sim, A. Larsson, P. Nordlund, *J. Biol. Chem.* **2017**, *8*, 53508.

SUPPORTING INFORMATION

Additional Supporting Information may be found online in the supporting information tab for this article.

How to cite this article: D. Insuasty, S. García, R. Abonia, B. Insuasty, J. Quiroga, M. Noguerras, J. Cobo, G. L. Borosky, K. K. Laali. Design, synthesis, and molecular docking study of novel quinoline-based bis-chalcones as potential antitumor agents. *Arch. Pharm.* 2021;e2100094. <https://doi.org/10.1002/ardp.202100094>